

# REMOVAL OF AMIDO BLACK DYE BY ADSORPTION WITH ZEOLITE SYNTHESIZED FROM FLY ASH

*Thesis submitted in partial fulfillment of the requirement  
for the award of the degree of*

*Master of Technology  
in  
Chemical Engineering*

Submitted By:

**Munish Mainrai**

Roll No.: 601011006

Under the Guidance of

**Dr. Sanghamitra Barman**  
Assistant Professor  
Dept. of Chemical Engg.

**Dr. Vijaya Kumar Bulasara**  
Assistant Professor  
Dept. of Chemical Engg.



**Department of Chemical Engineering  
Thapar University, Patiala**


Patiala-147004, Punjab, India

**July 2012**

# CERTIFICATE

*This is certified that the thesis entitled "Removal of Amido Black Dye by Adsorption with Zeolite synthesized from Fly Ash" is an authentic record of my own work carried out as requirements for the award of the degree of M.Tech (Chemical Engineering) at Thapar University, Patiala, under the guidance of Dr. Sanghamitra Barman (Assistant Professor, ChED) and Dr. Vijaya Kumar Bulasara (Assistant Professor, ChED) during January to June 2012.*

Date:- 13<sup>th</sup> July '12

  
Munish Mainrai  
Roll No. 601011006

It is certified that the above statement made by the student is correct to the best of our knowledge and belief.




**Dr. Sanghamitra Barman**  
Assistant Professor  
Department of Chemical Engineering  
Thapar University, Patiala



**Dr. Vijaya Kumar Bulasara**  
Assistant Professor  
Department of Chemical Engineering  
Thapar University, Patiala

Counter signed by:

  
13/7/12

**Dr. Rajeev Mehta**  
Head of the Department  
Department of Chemical Engineering



**Dr. S. K. Mohapatra**  
Dean of Academic Affairs  
Thapar University, Patiala

## ACKNOWLEDGEMENTS

At first, my heartfelt thanks to the almighty for his abundant blessing showered on me throughout this endeavor to complete the thesis work successfully. I am thankful to my parents for their great support throughout my life. I would cherish every moment where my parents were so keen and curious to know about the details and progress of my work, which boosted my confidence. I express my deep sense of gratitude to them.

I would like to thank **Dr. Sanghamitra Barman** for her valuable guidance and discussion regarding my work time to time.

My honorable guide **Dr. Vijaya Kumar Bulasara**, Assistant Professor, Department of Chemical Engineering, is a person to whom I shall always remain grateful for his excellent guidance, valuable discussions, encouragement, constructive criticism and his insights have strengthened this study significantly. He gave me a complete freedom to use my opinion, correcting whenever necessary in my dissertation.

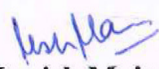
I am also thankful to **Mr. Abhishek Garg**, III year B.E student of Chemical Engineering for his significant contribution in the experimental work.

I would like to thank our Head of the Department, **Dr. Rajeev Mehta**, who has been supportive at all times and accommodative.

I thank my P.G. Coordinator, **Dr. Raj Kumar Gupta** for his useful suggestions regarding the thesis writing.

I would like to thank the most senior person, **Dr. P.K. Bajpai** (Distinguished Professor) for his guidance and blessings.

I would like to thank all my colleagues, faculty and staff of the department for their cooperation to carry out my research smoothly.

  
**Munish Mainrai**

## ABSTRACT

Investigations have been undertaken to determine whether zeolite synthesized from fly ash hold promise in the treatment of wastewater from the textile industry. The initial findings indicate that zeolite synthesized from fly ash has high adsorptive capacity for dyes and it is relatively cheap. This work presents the experimental studies on the adsorptive removal of Amido Black 10 B dye using a low-cost zeolite synthesized from fly ash. Preparation methodology for zeolite involved mixing of fly ash with NaOH, fusion of the mixture at 600°C, grinding, aging, curing, filtration, washing and drying. The synthesized zeolite was then used to study the effect of various parameters namely pH, temperature, agitation speed, adsorption time, zeolite loading and initial dye concentration on the dye removal efficiency. Then, the optimal process parameters for the dye–zeolite system were determined. Each experiment was carried out thrice and the average values were reported to ensure the consistency, repeatability and accuracy of the results. It was observed from the experimental analysis that the dye removal efficiency increases with increasing the adsorbent dosage, adsorption time as well as stirrer speed and the optimal values of zeolite dosage, adsorption time and stirrer speed were found to be 10 g/L, 6 h and 300 rpm respectively. On the other hand, the dye removal efficiency decreased with increasing the initial dye concentration in the solution as well as temperature, indicating that the adsorption process using zeolite is exothermic and is effective for the treatment of solutions with low concentrations of adsorbate. The effect of pH on the dye removal efficiency did not show any regular trend. A sudden drop in the removal efficiency from a pH of 6 to a pH of 8 was noticed. Maximum dye removal was obtained at low pH values (between 2–5) indicating the fact that the zeolite surface is positively charged. The spent adsorbent was regenerated by ultrasonic cleaning with surfactant solution followed by rinsing, drying and sintering. The regenerated zeolite performed in a way similar to the original zeolite with a little decrease in removal efficiency. Finally, the data were fitted with various equilibrium and kinetic models and the model parameters were obtained by curve fitting and regression analysis.

# CONTENTS

Chapter	Title	Page No.
	Abstract	i
	Contents	ii
	List of figures	iv
	List of Tables	vi
	Symbols/Abbreviations	vii
<b>1</b>	<b>Introduction</b>	<b>1</b>
	1.1 Zeolites	3
	1.2 Objectives of the present investigation	5
	1.3 Application of zeolites for the adsorption of dyes	5
<b>2</b>	<b>Literature Review</b>	<b>8</b>
	2.1 Literature on the zeolite as adsorbent	8
	2.2 Literature on the removal of Amido Black 10B	10
	2.3 Summary	12
<b>3</b>	<b>Experimental Methodology</b>	<b>13</b>
	3.1 Preparation of zeolite from fly ash	13
	3.2 Procedure for adsorption experiments	13
<b>4</b>	<b>Results and Discussion</b>	<b>16</b>
	4.1 Zeolite properties	16
	4.2 Zeolite synthesis conditions	16
	4.3 Zeolite characterization	16
	4.4 Determination of $\lambda_{\max}$ for Amido Black 10B	20
	4.5 Calibration curve for Amido Black 10B	21
	4.6 Adsorption experiments	22
	4.6.1 Effect of zeolite loading	23
	4.6.2 Effect of solution pH	25
	4.6.3 Effect of stirrer speed	27
	4.6.4 Effect of dye concentration	29

4.6.5 Effect of adsorption time	30
4.6.6 Effect of temperature	31
4.7 Thermodynamic, Kinetic and Equilibrium studies	33
4.7.1 Thermodynamics of adsorption	33
4.7.2 Adsorption Kinetics	34
4.7.3 Equilibrium Adsorption Isotherms	38
4.8 Comparison of zeolite performance with a commercial adsorbent	42
<b>5 Conclusions and Future Work</b>	<b>43</b>
<b>References</b>	<b>45</b>

---

## List of Figures

Figure	Title	Page No.
1.1	Primary building unit of zeolite structure	4
1.2	Structure of Amido Black 10B dye	6
3.1	Process diagram for zeolite synthesis	15
4.1	XRD of Commercial X zeolite	18
4.2	XRD of Synthesized zeolite ZX	18
4.3	SEM of synthesized zeolite ZX	19
4.4	A plot of absorbance versus wavelength for Amido Black 10B dye solution	20
4.5	Calibration curve for Amido black 10 B dye solution	21
4.6	Variation of dye removal efficiency with zeolite concentration	24
4.7	Variation of adsorption capacity with zeolite concentration	24
4.8	Variation of dye removal efficiency with pH	25
4.9	Variation of dye removal efficiency with stirrer speed	28
4.10	Variation of dye removal efficiency with initial dye concentration	29
4.11	Variation of dye removal efficiency with time	31
4.12	Variation of dye removal efficiency with temperature	32
4.13	Plot of change in Gibbs free energy with temperature	33
4.14	Pseudo first order kinetic model for the adsorption of Amido Black 10B dye on zeolite	35
4.15	Pseudo second order kinetic model for the adsorption of Amido Black 10B dye on zeolite	36
4.16	Intra particle diffusion model for the adsorption of Amido Black 10B dye on zeolite	37

4.17	Plot of $C_e/Q_e$ versus $C_e$ for the estimation of Langmuir Isotherm Constants	39
4.18	Variation of equilibrium adsorption density ( $R_L$ ) with initial dye concentration ( $C_i$ )	39
4.19	Equilibrium Isotherms for the adsorption of Amido Black dye on zeolite	40
4.20	Comparison of dye removal efficiency over synthesized zeolite (ZX) and Commercial Zeolite(13X)	42

---

## List of Tables

<b>Table</b>	<b>Title</b>	<b>Page No.</b>
1.1	Typical oxide formula of some synthetic zeolites	4
4.1	Synthesis conditions for zeolite ZX prepared from fly ash	16
4.2	Composition of different zeolites by EDAX	19
4.3	Calculation of dye removal efficiency from absorbance values at different zeolite dosage	23
4.4	Calculation of dye removal efficiency from absorbance values at different pH values	25
4.5	Calculation of dye removal efficiency from absorbance values at different stirrer speeds	27
4.6	Calculation of dye removal efficiency from absorbance values at different dye concentrations	29
4.7	Calculation of dye removal efficiency from absorbance values at different adsorption times	30
4.8	Calculation of dye removal efficiency from absorbance values at different temperatures	31
4.9	Equilibrium parameters for Langmuir and Freundlich adsorption isotherms	41

## List of Symbols/Abbreviations

---

$C_i$	initial dye concentration in the solution, mg/L
$C_f$	dye concentration in the solution after adsorption with zeolite, mg/L
$C_z$	zeolite loading (adsorbent dosage), g/L
R	dye removal efficiency, %
$q_t$	amount of dye adsorbed per unit weight of zeolite, mg/g
$\Delta G^\circ$	change in Gibbs free energy, J
$\Delta H^\circ$	change in enthalpy, J
$\Delta S^\circ$	change in entropy, J K <sup>-1</sup>
R	universal gas constant, J mol <sup>-1</sup> K <sup>-1</sup>
$q_e$	equilibrium dye adsorption capacity, mg/g
$k_1$	pseudo first-order rate constant, min <sup>-1</sup>
$k_2$	pseudo second-order rate constant, g.mg <sup>-1</sup> .min <sup>-1</sup>
$C_e$	liquid phase concentration of adsorbate at equilibrium, mg/L
$Q_m$	maximum adsorption capacity of the adsorbent, mg/g
$K_L$	equilibrium adsorption constant of the Langmuir isotherm, L/mg
$R_L$	equilibrium adsorption intensity
$K_F$	Freundlich constant, (mg/g).(mg/L) <sup>-n</sup>
n	exponent in Freundlich isotherm equation
$R^2$	correlation coefficient

---

Adsorption has been found to be superior to other techniques for water re-use in terms of initial cost, simplicity of design, ease of operation and insensitivity to toxic substances. Activated carbon is the most popular adsorbent and has been used with great success, but is expensive [Chakrabarty et al. 2003]. A full description of low cost adsorbents for waste and wastewater treatment: a review has been presented by S.J.T. [Yunus et al., 2006]. A number of studies have been reported with regard to the adsorption equilibrium of dye removal processes using various adsorbents. In most adsorption systems of dyestuffs-adsorbent, Langmuir [Elbec et al., 1985; Fatma et al., 2006; Venkat et al., 2006], Freundlich [Pollock et al., 1973], and Redlich-Peterson [Hou et al., 2000; Chakrabarty et al., 2003; Purkait et al., 2003] isotherms have been applied to describe equilibrium between liquid–solid phases. Two intraparticle diffusion mechanisms are involved in the adsorption rate (a) diffusion within the pore volume known as pore diffusion, and (b) diffusion along the surface of pores known as surface diffusion [Gong et al. 2005]. Some of the investigators have applied the pore diffusion model with and without film resistance. McKay has developed homogeneous solid phase diffusion model to describe systems dyes on bagasse pith [Purkait et al., 2003]. The homogeneous solid phase diffusion model has been developed based on external mass transfer and surface diffusion by M.S.El-Geundi [Hau et al., 2000]. He has applied this model for adsorption of basic dyes onto natural clay in a batch adsorber. The branched pore kinetic model was used to describe the adsorption of cobalt phthalocyanine dye onto active carbon and basic dyes onto natural clay [Pollock et al., 1973].

Research has already been carried out using different treatment technologies e.g. chemical coagulation-flocculation, different types of oxidation processes, biological processes [Ledakowicz et al., 2001], membrane based separation processes [Dey et al., 2006], adsorption [Dasgupta et al., 2006] etc. for the removal of colored dye from wastewater. Each of the above processes has its own benefits and limitations. Adsorption on solid surface is of growing interest in this field because of its lower price. Activated carbon is one of the common adsorbents due to its high surface area and high adsorption capacity. However, its high cost makes the process uneconomical

for industrial applications. Therefore, the process of dye removal by adsorption is being diverted to the use of lower cost adsorbents so that the process becomes economically feasible.

For this reason, research is focused on the use of low-cost, reusable, locally available, biodegradable adsorbents made from natural sources. Zeolite synthesized from fly ash is being considered as alternative low-cost adsorbents. Adsorption of organic molecules to an adsorbent depends on various factors like temperature, pH of the solution, the structure and concentration of the adsorbing molecule, the ionic strength of the suspension, and the structure of the adsorbent.

However, adsorption over a surface with highly ionic character is mostly effective and very fast for a dye with opposite ionic character. Although very few works have been done on adsorption of dyes on zeolite, the present work gives detailed information about the adsorption of Amido Black 10B on zeolite synthesized from fly ash. Very scarce literature is available on the adsorption of Amido Black dye. Adsorption experiments using zeolite as an adsorbent were carried out by Sakti et al. (2011) on different basic and acidic dyes such as Methylene Blue, Methyl Orange etc. They observed the usability of zeolite as an adsorbent for the removal of acidic and basic dyes only. Systematic experimentations that include characterization of adsorbent, stirring effect, role of pH, temperature, and the dose of the adsorbent as well as the adsorbate are yet to be done. Again, determination of various thermodynamic parameters, kinetic and equilibrium model parameter will also be the further scope of research.

The aim of this work is to study the ability of zeolite synthesized from fly ash to remove the acidic dye Amido Black 10B from aqueous solutions. This adsorbent was chosen because of its cheapness and abundance. The equilibrium isotherms and the kinetics for these systems have to be determined. The importance of such isotherms and kinetics curves lies in developing a model, which accurately represents both the obtained results, and could be used for design purposes.

Fly ash, an oxide-rich waste product of thermal power plants, can be used as raw material for different industries on proper treatment. In India, a little effort has been paid on proper utilization of fly ash. However, only three percent of fly ash is being

utilized, mostly in the manufacture of pozzolonic cement, ready-made hollow blocks, and asbestos sheets and in road embankment and agricultural purpose.

Two classes of fly ash are defined by American Society of Testing Material (ASTM):

- Class F fly ash
- Class C fly ash

#### **Class F fly ash:**

The burning of harder, older anthracite and bituminous coal typically produces Class F fly ash. This fly ash is pozzolanic in nature, and contains less than 20% lime (CaO). Possessing pozzolanic properties, the glassy silica and alumina of Class F fly ash requires a cementing agent, such as Portland cement, quicklime, or hydrated lime, with the presence of water in order to react and produce cementitious compounds. Alternatively, the addition of a chemical activator such as sodium silicate (water glass) to a Class F ash can lead to the formation of a geopolymer.

#### **Class C fly ash:**

Fly ash produced from the burning of younger lignite or sub bituminous coal, in addition to having pozzolanic properties, also has some self-cementing properties. In the presence of water, Class C fly ash will harden and gain strength over time. Class C fly ash generally contains more than 20% lime (CaO). Unlike Class F, self-cementing Class C fly ash does not require an activator. Alkali and sulfate (SO<sub>4</sub>) contents are generally higher in Class C fly ashes.

### **1.1 Zeolites**

The types of zeolites formed on treatment are very much selective to reaction parameters and also the raw material compositions. The synthesis of various zeolite from fly ash and their properties mainly depend on the effect of reaction time, reaction temperature, alkalinity and fly ash composition.

Zeolites are crystalline, micro-porous, hydrated aluminosilicates that are built from an infinitely extending three-dimensional network of [SiO<sub>4</sub>]<sup>4-</sup> and [AlO<sub>4</sub>]<sup>4-</sup> tetrahedral linked to each other by the sharing of oxygen atom. Generally, their structure can be considered as inorganic polymer built from tetrahedral TO<sub>4</sub> units, where T is Si<sup>4+</sup> or Al<sup>3+</sup> ion. Each oxygen (O) atom is shared between two T atoms.

$M_{x/n}[(AlO_{2x}(SiO_2)_y) \cdot wH_2O]$ , where M is an alkali or alkaline earth cation, n is the valence of the cation, w is the number of water molecules per unit cell, x and y are the total number of tetrahedra per unit cell, and the ratio y/x usually has values of 1 to 5, though for the silica zeolite, y/x can be ranging from 10 to 100.

The adsorption of dyes onto zeolites has been extensively investigated by some researcher but only a few studies have been reported about the adsorption of dye onto fly ash-based zeolites. A comparison of the adsorption capabilities of zeolite synthesized from fly ash and that of commercial zeolite has been investigated with adsorption kinetics.

### 1.1.1 Structure of Zeolite

The primary building unit for zeolites is the tetrahedron and the secondary building units (SBUs) are the geometric arrangements of tetrahedra. The SBUs may be simple polyhedra such as cubes, hexagonal prisms, or cubo-octahedra. The structures can be formed by repeating SBUs.

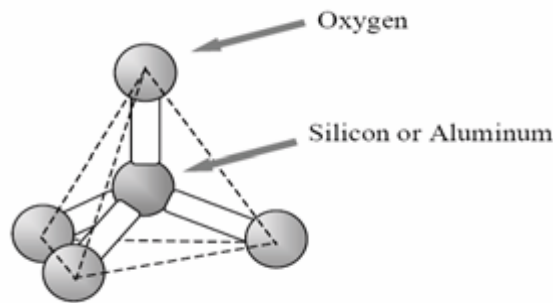


**Figure 1.1:** Primary building unit of zeolite structure

### 1.1.2 Types of zeolite

The following table presents the most common types of zeolites.

<b>Zeolites</b>	<b>Typical oxide formula</b>
Zeolites A	$Na_2O \cdot Al_2O_3 \cdot 2SiO_2 \cdot 4.5H_2O$
Zeolites X	$Na_2O \cdot Al_2O_3 \cdot 2.5SiO_2 \cdot 6H_2O$
Zeolites Y	$Na_2O \cdot Al_2O_3 \cdot 4.8SiO_2 \cdot 8.9H_2O$

**Table 1.1** Typical oxide formula of some synthetic zeolites

## 1.2 Objectives of the present study

The objectives of the present investigations are

- Synthesis of Zeolite from Fly ash
- Characterization of synthesized zeolite by XRD,SEM/EDAX and BET apparatus
- Carrying out adsorption experiments and study the effects of initial dye concentration, contact time, zeolite loading, stirring speed, pH, and temperature for the adsorption of Amido Black 10B over synthesized zeolite in batch mode.
- Thermodynamic study of adsorption
- To study the adsorption kinetics using various kinetic models
- Comparison of adsorption capacity of low cost zeolite synthesized from fly ash with that of Commercial zeolite

## 1.3 Application of zeolites for the adsorption of dye

Adsorption processes are important fields of study in physical chemistry. They form the basis for understanding phenomena such as adsorbent, heterogeneous catalysis, chromatographic analysis, dyeing of textiles, and clarification of various effluents.

Dyes are defined as colored substances which when applied to fibers give them a permanent color, i.e. resistant to action of light, water and soap. Practically every dyestuff is made from either one or more of the compounds obtained by the distillation of the coal tar. The chief of these are Benzene ( $C_6H_6$ ), Toluene ( $C_6H_5.CH_3$ ), Naphthalene ( $C_{10}H_8$ ), Anthracene ( $C_{14}H_{10}$ ), Phenol ( $C_6H_5OH$ ), Cresol ( $C_7H_7OH$ ), Acridine ( $C_{13}H_9N$ ), and Quinoline ( $C_9H_7N$ ).

Wastewaters from dyeing and finishing operations in the textile industry are generally high in both color and organic content. Color removal from textile effluent has been the target of great attention in the last few years, not only because of its potential toxicity, but also mainly due to its visibility problems. Recent estimate indicates that 20% of dyes enter the environment through effluent that result from the treatment of industrial wastewater. The existing technologies have certain efficiency in the removal of dyes but their initial and operational costs are very high. On the other hand, low cost

technologies do not allow the desired degree of color removal or have certain disadvantage.

Oxidation and adsorption are two major technologies that are used for wastewater treatment in the textile industry. Among oxidation methods, UV/Ozone and UV/H<sub>2</sub>O<sub>2</sub> treatments are technologies for decolorizing wastewater. Adsorption is rapidly becoming a prominent method of treating aqueous effluents and it has been extensively used in industrial processes for a variety of separation and purification purposes. Adsorption of dyes by zeolites has evolved into one of the most effective physical process for the decolorization of textile wastewater. This process has been found to be superior to other techniques for water re-use in terms of initial cost, simplicity of design, ease of operation and insensitivity to toxic substances.

### 1.3.1 Amido Black dye

Amido black 10B is an amino acid staining diazo dye. Its molecular formula is C<sub>22</sub>H<sub>14</sub>N<sub>6</sub>Na<sub>2</sub>O<sub>9</sub>S<sub>2</sub>. Amido Black 10B is a synthetic acid dye containing both NN and CC chromophore groups (pyrazolone dye). It is a dark red to black powder soluble in water and used as a stain for protein-containing. Its chemical designation is 4-amino-5-hydroxy-3-[(4-nitrophenyl)azo]-6-(phenylazo)-2,7-naphthalene disulfonic acid disodium salt. Acid dyes are water-soluble dyes employed mostly in the form of sodium salts of the sulfonic or carboxylic acids. They are anionic which attach strongly to cationic groups in the fibre directly. They can be applicable to all kind of natural fibres like wool, cotton and silk as well as to synthetics like polyesters, acrylic and rayon. However, they are not substantive to cellulosic fibres. They are also used in paints, inks, plastics and leather. Chemical structure of Amido Black dye is given below.

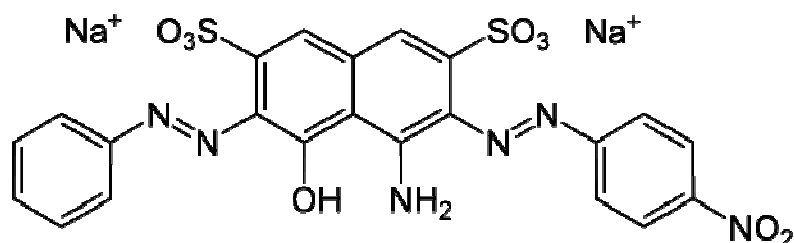


**Figure 1.2:** Structure of Amido Black 10B dye

Zeolitized fly ash product is successfully used as low cost adsorbent for this anionic dye. Equilibrium and kinetic results obtained in this study may be useful for designing a treatment plant for dye removal from industrial colored effluents.

### 2.1 Zeolite as adsorbent

Recent investigations have shown the potential of fly ash as a raw material for synthesis of various types of zeolites. The conversion of fly ash to zeolite has gained importance due to intensive research on zeolite and growth in geological materials such as volcanic rock and clay minerals. High content of reactive materials like aluminosilicate makes it an interesting starting material for the synthesis of zeolite with a wide range of applications. Various methods of synthesis of zeolite from fly ash have, so far, been invented and patented. Some of the important techniques are alkali fusion followed by hydrothermal treatment (Shigemoto et al., 1993), slurry method (Grutzeck & Siemer, 1997), molten salt method (Park et al., 2000a, 2000b). Fusion method is found to be the most efficient and a general method for synthesis of X-type, Y-type, and A-type from a large variety of fly ash.

A modified fusion process to synthesize X from fly ash was studied by Chang et al. (2000). It was found that the addition of aluminium hydroxide to the fused fly ash solution followed by hydrothermal treatment at 60 °C produced single phase zeolite A and X depending on the source of the ash received fly ash. The result confirms that the quantity of dissolved aluminium species is critical for the type of zeolite formed from fused fly ashes.

Sutarno et al. (2007) synthesized faujasite from fly ash and its application for hydrocracking catalyst of heavy petroleum distillates has been studied. Faujasite was synthesized from fly ash by hydrothermal reaction in alkaline solution via combination of reflux treatment of fly ash with HCl and fusion with NaOH.

Ojha et al. (2004) synthesized X-type zeolite by alkali fusion followed by hydrothermal treatment. The synthesized zeolite was characterized using various techniques such as X-ray diffraction, scanning electron microscopy, Fourier transform infrared spectroscopy.

Querol et al. (2002) synthesized zeolitic material from fly ash using two different methodologies: (a) impure zeolitic material obtained by direct conversion from

different fly ashes, and (b) a high purity 4A-X zeolite blend synthesized from the silica extracts obtained from the Meirama fly ash.

Lu et al. (2010) synthesized zeolite NaPI by a hydrothermal method from coal fly ash, the possibility of using modified zeolite NaPI as a material for removing fluorine from drinking water was studied.

Fukui et al. (2003) studied the effects of NaOH concentration on the crystal structure and the reaction rate of zeolite synthesized from fly ash with a hydrothermal treatment.

Rungsuk et al. (2006) synthesized zeolite by fusion method. The synthesis conditions were optimized to obtain the product with high cation exchange capacity (CEC). CFA was mixed with NaOH at various ratios and the results revealed that the optimal ratio between CFA and NaOH.

Vadapalli et al. (2010) studied solid residues resulting from the active treatment of acid mine drainage with coal fly ash were successfully converted to zeolite-P under mild hydrothermal treatment conditions. Scanning electron microscopy showed that the zeolite-P product was highly crystalline. The product had a high cation exchange capacity (178.7 meq / 100 g) and surface area (69.1 m<sup>2</sup>/g) and has potential application in wastewater treatment.

Sutarno et al. (2007) synthesized faujasite from fly ash and its application for hydrocracking catalyst of heavy petroleum distillates has been studied. Faujasite was synthesized from fly ash by hydrothermal reaction in alkaline solution via combination of reflux treatment of fly ash with HCl and fusion with NaOH.

Ojha et al. (2004) synthesized X-type zeolite by alkali fusion followed by hydrothermal treatment. The synthesized zeolite was characterized using various techniques such as X-ray diffraction, scanning electron microscopy, Fourier transform infrared spectroscopy.

Querol et al. (2002) synthesized zeolitic material from fly ash using two different methodologies.(a) impure zeolitic material obtained by direct conversion from different fly ashes, and (b) a high purity 4A-X zeolite blend synthesized from the silica extracts obtained from the Meirama fly ash.

Lu et al. (2010) synthesized zeolite NaPI by a hydrothermal method from coal fly ash, the possibility of using modified zeolite NaPI as a material for removing fluorine from drinking water was studied.

Fukui et al. (2003) studied the effects of NaOH concentration on the crystal structure and the reaction rate of zeolite synthesized from fly ash with a hydrothermal treatment.

Rungsuk et al. (2006) synthesized zeolite by fusion method. The synthesis conditions were optimized to obtain the product with high cation exchange capacity (CEC). CFA was mixed with NaOH at various ratios and the results revealed that the optimal ratio between CFA and NaOH.

## **2.2 Literature on the removal of Amido Black 10B**

Very less work has been investigated for the removal of amido black and thionin by zeolite. Only few studies have been reported for this dye. However, zeolite and other adsorbents such as activated carbon and fly ash have been investigated extensively.

Recently, Senthilkumar et al. (2011) investigated the decolourization potential of white-rot fungus *Phanerochaete chrysosporium*, which is capable of decolourizing synthetic dye bath effluent containing Amido Black 10B. Need of additives such as enzymes and nutrients and inducers such as starch and lignin during the digestion of dye makes the process highly expensive. Although they are capable of removing the dye up to 98% within 7–10 days, it is still a time consuming process.

Ahmad and Kumar (2010) prepared a novel adsorbent polyaniline/iron oxide composite and evaluated its dye adsorption characteristics for aqueous solution of Amido Black 10B. They described the kinetic data successfully in terms of pseudo-first-order and pseudo-second-order kinetic models. The adsorption equilibrium data fitted well with the Freundlich isotherm than the Langmuir isotherm.

Qiu et al. (2009) studied the adsorption of Amido Black 10B and Safranin T dyes onto a natural zeolite *clinoptilolite*. They analyzed the influence of adsorbent concentration, adsorption time, initial dye concentration, and pH on the dye adsorption capacity. They varied the zeolite loading from 0–160 g/L and the dye concentration from 0–40 mg/L. They obtained a maximum removal efficiency of 81.2% for Safranin T and 16.3% for Amido Black. Their observation indicates that clinoptilolite

has a limited adsorption capacity for Amido Black dye. They found that these dye-zeolite systems fitted perfectly to the Langmuir isotherm.

Sun et al. (2006) investigated degradation of azo dye Amido black 10B in aqueous solution by Fenton oxidation process.

Liu and Zhang (2007) studied Adsorption of organic dyes from aqueous solutions or suspensions with clay nano-adsorbents.

Atun et al. (2011) investigated the adsorption characteristics of two basic dyes, thionine and safranine onto fly ash and its three zeolitized products prepared at different hydrothermal conditions.

Yasin et al. (2009) investigated on the removal of Amido Black dye from aqueous solution by uncalcined and calcined hydrotalcite.

Li et al. (2006) performed experiment for photocatalytic degradation of methyl orange by TiO<sub>2</sub>-coated activated carbon and kinetic study.

Mohammadi et al. (2011) studied adsorption process of methyl orange dye onto mesoporous carbon material—kinetic and thermodynamic studies.

Mittal et al. (2007) studied on the adsorption kinetics and isotherms for the removal and recovery of Methyl Orange from wastewaters using waste materials.

Chen et al. (2009) investigated equilibrium and kinetic studies of methyl orange and methyl violet adsorption on activated carbon derived from *Phragmites australis*.

Rafatullah et al. (2009) presented a review on the adsorption of methylene blue with low-cost adsorbents.

Han et al. (2007) investigated on the adsorption of methylene blue on to natural zeolite and studied about the equilibrium, kinetic and thermodynamic parameters.

Jin et al. (2008) studied adsorption of methylene blue and orange II onto unmodified and surfactant-modified zeolite.

Wang et al. (2005) used unburned carbon as a low-cost adsorbent for treatment of methylene blue-containing wastewater.

Dural et al. (2011) conducted kinetic and equilibrium studies on Methylene blue adsorption on activated carbon prepared from *Posidonia oceanica* (L.) dead leaves.

Kumar et al. (2004) modeled the mechanism involved during the adsorption of methylene blue onto fly ash.

Lin et al. (2007) studied adsorption of basic dye from aqueous solution onto fly ash.

Wang et al. (2008) studied characteristics of coal fly ash and adsorption application.

### **2.3 Summary**

Of these literatures, adsorptive removal of Amido Black using zeolite studied by Qiu et al. (2009) seems to be more relevant compared to others. The main drawback of their study is that they could not remove Amido Black dye more than 16.3%, which indicates that a suitable low-cost adsorbent for effective removal of Amido Black dye from its aqueous solution needs to be investigated.

### 3.1 Zeolite synthesis

Before any treatment, the raw fly ash samples were first screened through a BSS Tyler sieve of 80-mesh size to eliminate the larger particles. The unburnt carbon (4–6%) along with other volatile materials present in fly ash were removed by calcination at  $800 (\pm 10) ^\circ\text{C}$  for 2 h. Mixture of sodium hydroxide and fly ash (calcined and HCl treated) in a pre-determined ratio, was milled and fused in a stainless steel tray at different temperatures ranging from  $500\text{--}650^\circ\text{C}$  for 1 h. The sodium hydroxide to fly ash ratio (by weight) was varied from 1–1.5. The resultant fused mixture was then cooled to room temperature, ground further and added to water (10 g fly ash/100 ml water). The slurry thus obtained was agitated mechanically in a glass beaker for several hours. It was then kept at around  $90^\circ\text{C}$  for 6 h without any disturbance. The flow diagram of the synthesis process is shown in Figure 3.1. The resultant precipitate was then repeatedly washed with distilled water to remove excess sodium hydroxide, filtered and dried. The sodium hydroxide added to the fly ash not only works as an activator, but also adjusts the sodium content in the starting material.

### 3.2 Procedure for adsorption experiments

Procedure for adsorption experiments for the removal of Amido Black dye using zeolite consist of the following steps.

- i) A 100 ml of standard dye solution (20 mg/L) is freshly prepared by mixing the required amount of Amido Black 10B powder in distilled water in a 250 ml beaker.
- ii) The pH of the solution is checked and adjusted to 3 by adding a few drops of standard HCl/NaOH solution.
- iii) A 2.5 g of zeolite is then added into the beaker containing the dye solution and it is well mixed.
- iv) Adsorption is carried out for 6 hours at ambient temperature ( $20^\circ\text{C}$ ) under continuous agitation at 125 rpm.

- v) The zeolite is then allowed for 30 min. to settle down and the solution is carefully separated from the zeolite.
- vi) The collected sample after adsorption is then analyzed by UV-Visible spectrophotometer and the absorbance value is noted down.
- vii) The above procedure is repeated by adding different amounts of zeolite (in step ii).
- viii) These absorbance values are matched with the corresponding calibration curve to obtain the dye concentration in the solution after adsorption with zeolite.
- ix) Dye removal efficiency and the adsorption capacity of the zeolite are calculated by using equations (4.1) and (4.2).

**Adsorption analysis was done by the Spectrophotometer:** A spectrophotometer is a photometer (a device for measuring light intensity) that can measure intensity as a function of the light source wavelength. Important features of spectrophotometers are spectral bandwidth and linear range of absorption or reflectance measurement. The spectrophotometer is commonly used for the measurement of transmittance or reflectance of solutions, transparent or opaque solids, such as polished glass, or gases. However, they can also be designed to measure the absorbance on any of the listed light ranges that usually cover around 200–2500 nm using different controls and calibration. Within these ranges of light, calibrations are needed on the machine using standards that vary in type depending on the wavelength of the photometric determination. The position of maximum absorbance ( $\lambda_{\max}$ ) of Amido Black 10B solution was determined to be at 618 nm on a spectrophotometer.

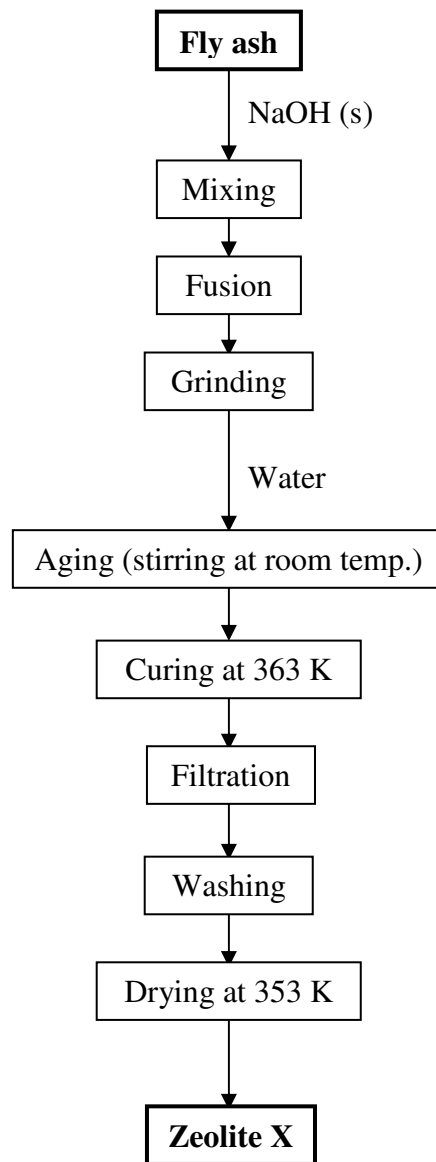


**Figure 3.1:** Process diagram for zeolite synthesis

## Chapter 4

## RESULTS AND DISCUSSION

---

### 4.1 Zeolite Properties

Zeolite was synthesized from fly ash using hydrothermal treatment. The synthesized Zeolite ZX is having the following properties given below.

- Particle size: 1–1.15 mm
- Porosity: 0.29
- Surface area: 485 m<sup>2</sup>/g

### 4.2 The synthesis conditions of zeolite ZX prepared from fly ash

The synthesis conditions for the preparation of zeolite ZX are presented in the following table.

**Table 4.1:** Synthesis conditions of zeolite ZX

Zeolite Designation	ZX
Source of fly ash	NTPC
NaOH/Fly ash ratio	1.3
Fusion Temp (K)	823
Aging Time (h)	24
Hydrothermal Treatment	
Temperature (K)	363
Time (h)	6

### 4.3. Zeolite characterization

#### 4.3.1 X-ray diffraction

The X-ray (powder) diffraction (XRD) patterns of commercial zeolite and synthetic zeolitic material synthesized from fly ash were obtained using a Philips X-ray diffractometer (Philips BW1710) and shown in Figure 4.1 and Figure 4.2. Operating conditions involved the use of CoK $\alpha$  radiation at 4 kV and 30 mA. The samples were scanned from 10–50° (2 $\theta$ , where  $\theta$  is the angle of diffraction). Various crystalline phases present in the samples were identified with the help of JCPDS

(Joint Committee on Powder Diffraction Standards) files for inorganic compounds. Quantitative measure of the crystallinity of the synthesized zeolite was made by using the summed heights of major peaks in the X-ray diffraction pattern (Szostak 1976). The major peaks were selected specifically because they are least affected by the degree of hydration of samples and also by others. The percentage crystallinity was taken as the sum of the peak heights of the unknown materials divided by the sum of the peak heights of a standard material that has been assume to be 100% crystalline i.e.

$\% \text{ Crystallinity} = (\text{sum of the peak heights of unknown material}) \times 100 / (\text{sum of peak heights of standard material}).$

#### **4.3.2. Particle size and surface area:**

The average particle sizes of various samples were determined by particle size analyzer (Malvern Instruments M7). BET method is used to measure specific surface area of the samples (Flowsorb-II, Micromeritics).

#### **4.3.3 Morphological analysis by scanning electron microscope (SEM):**

The morphological structure of the raw fly ash, synthesized zeolitic materials were obtained by using scanning electron micrograph (Jeol, JSM 5800) and is shown in Figure 4.3. The bulk composition was also estimated from SEM/EDXS by indirect method. The elemental composition of the samples was first determined from the SEM/ EDXS, the percentages of oxides were calculated. The results are shown in Table 4.2.

#### **4.3.4 BET Surface area**

The surface areas of zeolite ZX were measured by BET method (Flowsorb-II, Micromeritics, 230-000000-00, Nor Cross, GA, USA). The BET surface area of zeolite is reported in Table 4.2.

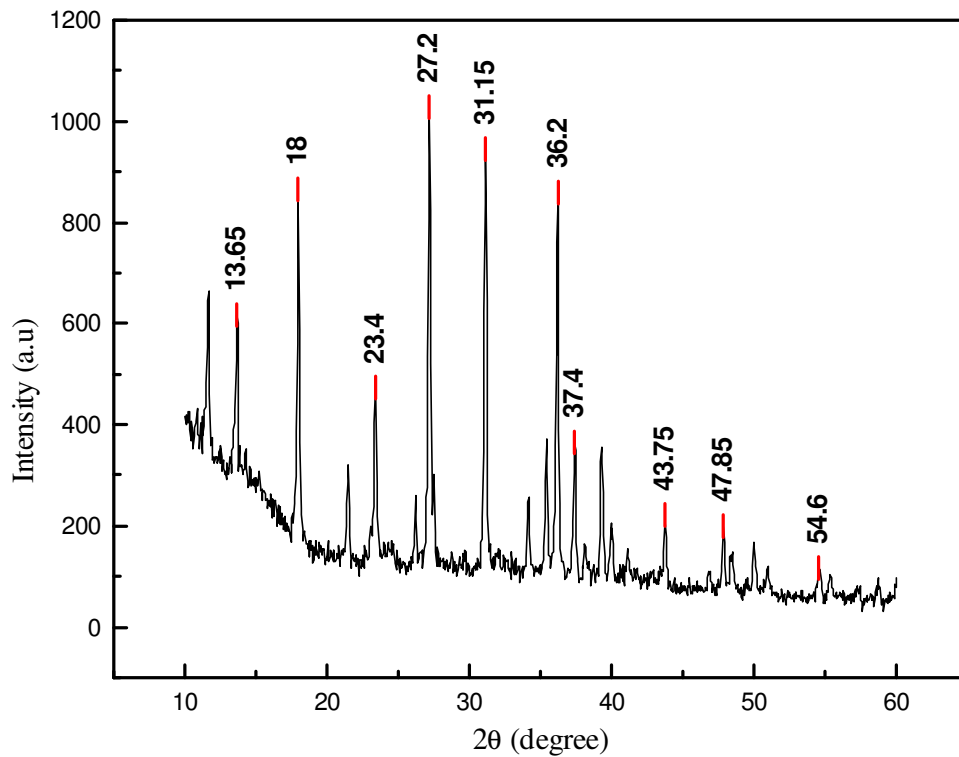


**Figure 4.1:** XRD of Commercial X zeolite

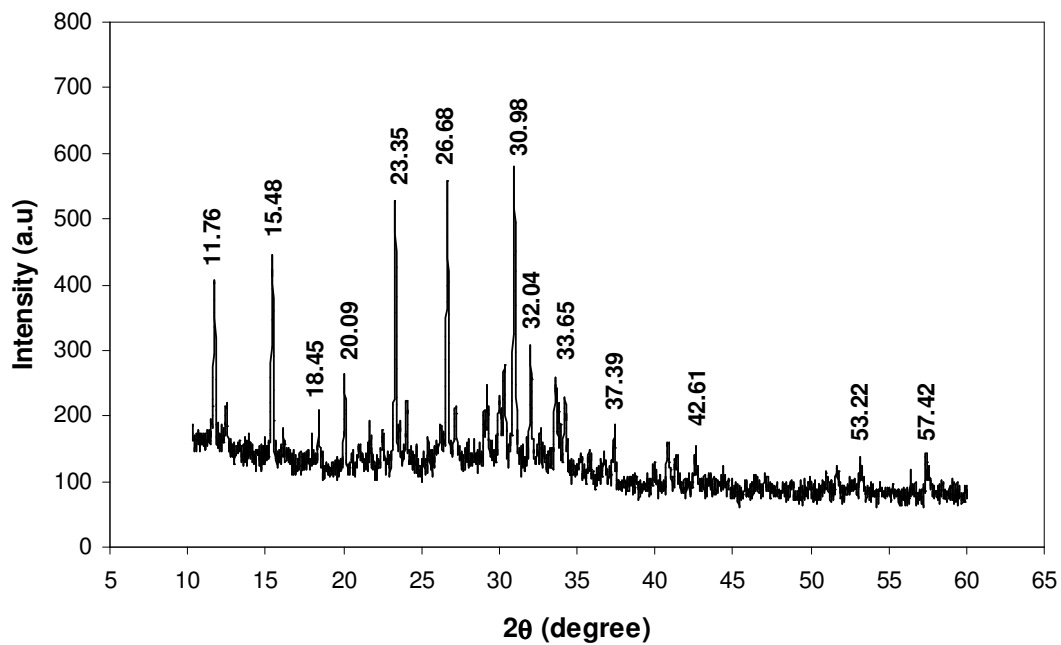


**Figure 4.2:** XRD of Synthesized zeolite ZX

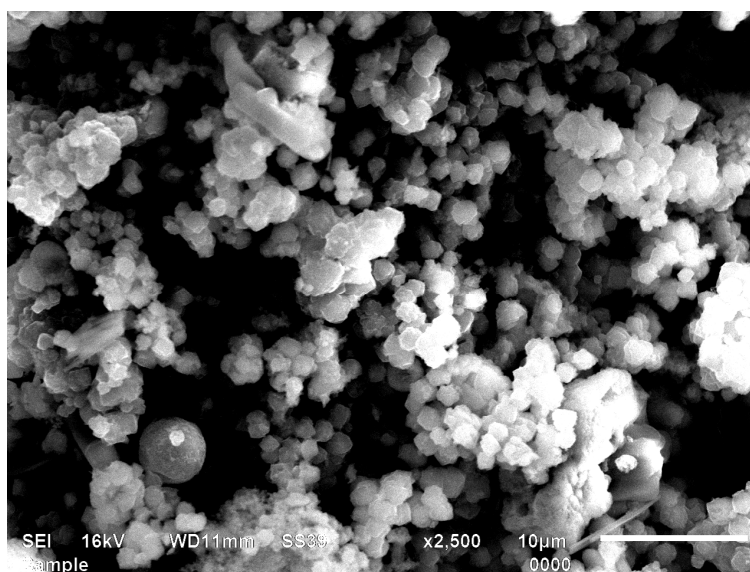


**Figure.4.3:** SEM of synthesized zeolite ZX

**Table.4.2:** Composition of different zeolite by EDAX

Composition (wt %)	NaX	Synthesized zeolite ZX
SiO <sub>2</sub>	48.26	49.21
Al <sub>2</sub> O <sub>3</sub>	31.87	32.33
Fe <sub>2</sub> O <sub>3</sub>	3.17	2.13
Na <sub>2</sub> O	15.67	14.34
CeO <sub>2</sub>	0.00	0.0
K <sub>2</sub> O	0.07	1.05
BaO	0.00	0.17
CaO	0.45	0.65
SO <sub>3</sub>	0.51	0.12
BET Surface area (m <sup>2</sup> /g)	478	485

#### 4.4 Determination of $\lambda_{\max}$ for Amido Black dye solution

To determine the wavelength that corresponds to maximum absorbance ( $\lambda_{\max}$ ), a standard solution of Amido Black in distilled water was scanned through a wavelength range of 200–700 nm using a UV–Visible spectrophotometer. Maximum absorbance value was noticed at a wavelength of 618 nm (Figure 4.4). The same value was also used in several literatures (Qiu et al., 2009). Therefore,  $\lambda_{\max}$  for amido black was taken as 618 nm.

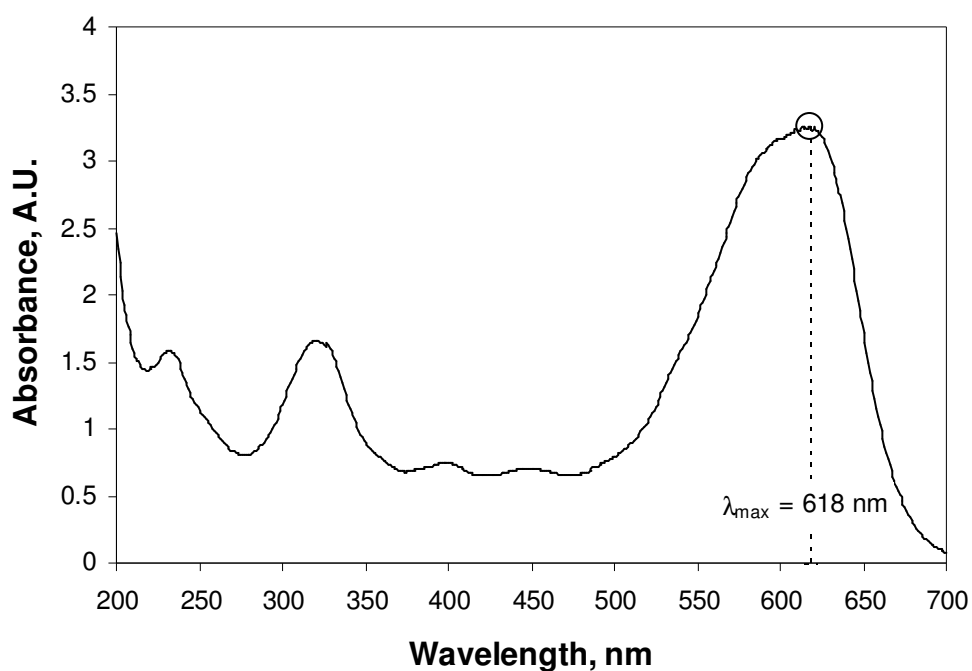


**Figure 4.4:** A plot of absorbance versus wavelength for Amido Black dye solution

#### 4.5 Calibration curve for Amido Black dye solution

Absorbance values were determined at various known concentrations of the dye solution to obtain a calibration curve for Amido Black dye solution. As shown in Figure 4.5, a linear fit to the observed data (absorbance versus dye concentration) yielded a straight line with a slope of 0.0658. This calibration curve can be used for the determination of unknown dye concentration in the solution after adsorption with zeolite.

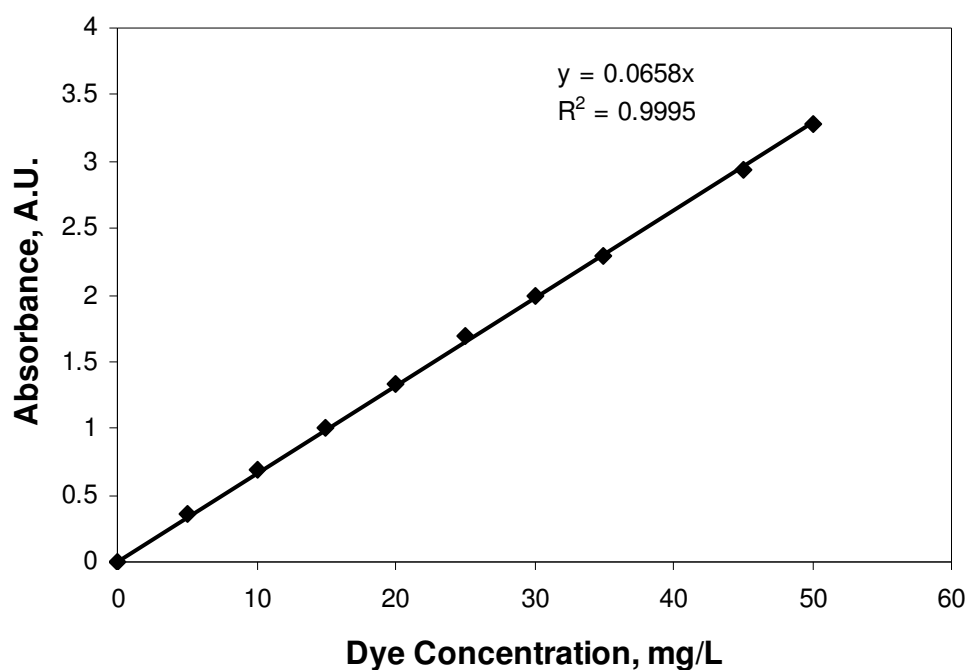


**Figure 4.5:** Calibration curve for amido black dye solution

## 4.6 Adsorption experiments

The adsorbent used in the experiment was zeolite (ZX) synthesized from fly ash. The adsorption experiments were carried out for 6 h under continuous agitation at 125 rpm and 20°C to remove Amido black 10B dye from its aqueous solution. Effect of dye concentration on the removal efficiency was studied using different dye concentrations in the range of 0–50 mg/L.

Dye removal efficiency was determined from the dye concentration in the solution before and after adsorption with zeolite.

$$\text{Removal efficiency, } R = \left( \frac{C_i - C_f}{C_i} \right) \times 100 \quad (4.1)$$

$$\text{Adsorption capacity, } q_t = \frac{C_i - C_f}{C_z} \quad (4.2)$$

Here,

$C_i$  = initial dye concentration in the solution, mg/L

$C_f$  = dye concentration in the solution after adsorption with zeolite, mg/L

$C_z$  = zeolite loading (adsorbent dosage), g/L

$q_t$  = amount of dye adsorbed per unit weight of zeolite, mg/g

#### 4.6.1 Effect of zeolite dosage

The values of dye removal efficiency and adsorption capacity of zeolite evaluated using the above formulae (Eq. 4.1–4.2) for various concentrations of zeolite were presented in Table 4.3.

**Table 4.3:** Calculation of dye removal efficiency from absorbance values

<b>Zeolite concentration</b> (g/L)	<b>Absorbance value</b> (A.U.)	<b>Solution concentration</b> (mg/L)	<b>Removal efficiency</b> (%)	<b>Adsorption capacity</b> (mg/g)
0	1.330	20.2	0	–
2.5	0.954	14.5	28.3	2.3
5	0.600	9.1	54.9	2.2
7.5	0.425	6.5	68.0	1.8
10	0.348	5.3	73.8	1.5
12.5	0.359	5.5	73.0	1.2
15	0.320	4.9	75.9	1.0

A plot of dye removal efficiency versus zeolite concentration yielded a non-linear profile as shown in Figure 4.6. From this figure, it can be observed that the removal efficiency increased with increasing the zeolite concentration up to 10 g/L and no significant improvement in the removal efficiency values was observed beyond this value. Hence, the optimal zeolite concentration for the removal of Amido Black dye was chosen to be 10 g/L. Similar observation was reported by Qiu et al. (2009). However, the authors were able to obtain a dye removal efficiency of 16.3% for the removal of Amido Black 10B using a natural zeolite clinoptilolite. Hence, it can be concluded that the zeolite synthesized from fly ash is far better than clinoptilolite.

Initially, rapid increase in the adsorption with the increase in the adsorbent dose can be attributed to a greater surface area and availability of more adsorption sites. After this critical dose (10 g/L) the extent of adsorption is increasingly slowed down due to the fact that although there is increasing number of active sites but there is shortage of adsorbate in the solution.

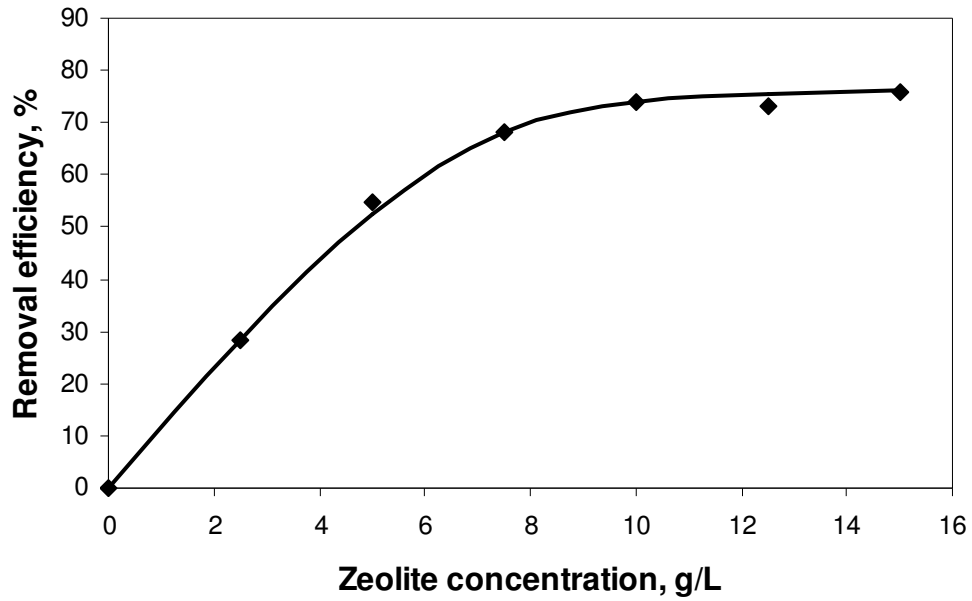


**Figure 4.6:** Variation of dye removal efficiency with zeolite concentration

As can be seen from Figure 4.7, the adsorption capacity of the zeolite (determined by Eq. (4.2)) decreased with increasing the zeolite concentration. It indicates that the adsorption capacity of a zeolite decreases with increasing the zeolite dosage. Hence, it can be concluded that too much of zeolite concentration in the solution is not effective for adsorption and is also not economical.

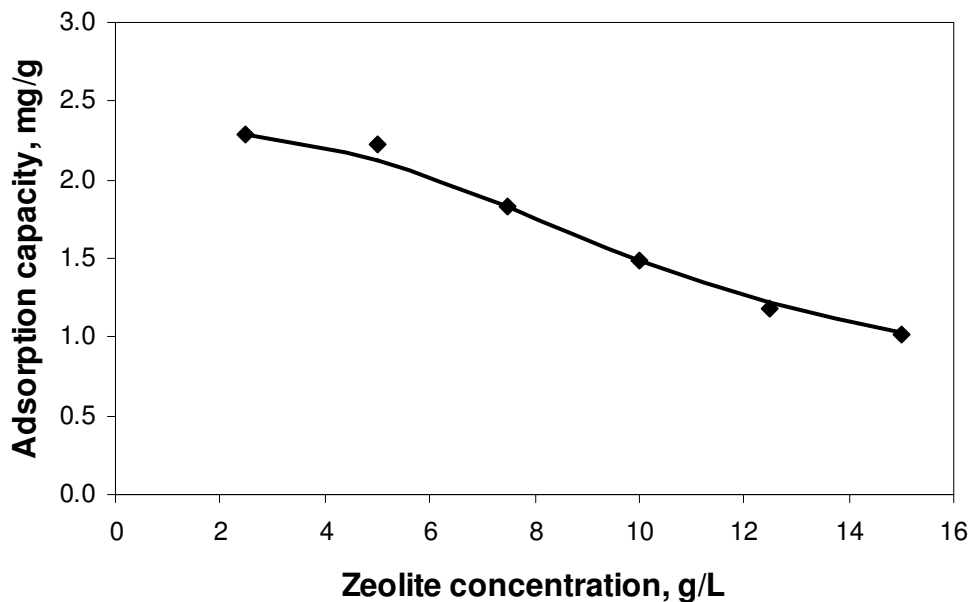


**Figure 4.7:** Variation of adsorption capacity with zeolite concentration

#### 4.6.2 Effect of solution pH

To study the effect of solution pH on the dye removal efficiency, adsorption experiments were conducted at various pH values between 2 and 12. The values of dye removal efficiency for various pH values are presented in Table 4.4 and the corresponding plot of dye removal efficiency versus pH is shown in Figure 4.8.

**Table 4.4:** Calculation of dye removal efficiency from absorbance values

pH	Absorbance value (A.U.)	Solution concentration (mg/L)	Removal efficiency (%)
2	0.340	5.2	74.2
3	0.341	5.2	74.1
4	0.342	5.2	74.0
5	0.374	5.7	71.6
6	0.397	6.0	69.8
7	0.512	7.8	61.1
8	0.651	9.9	50.5
10	0.698	10.6	47.0
12	0.722	11.0	45.1

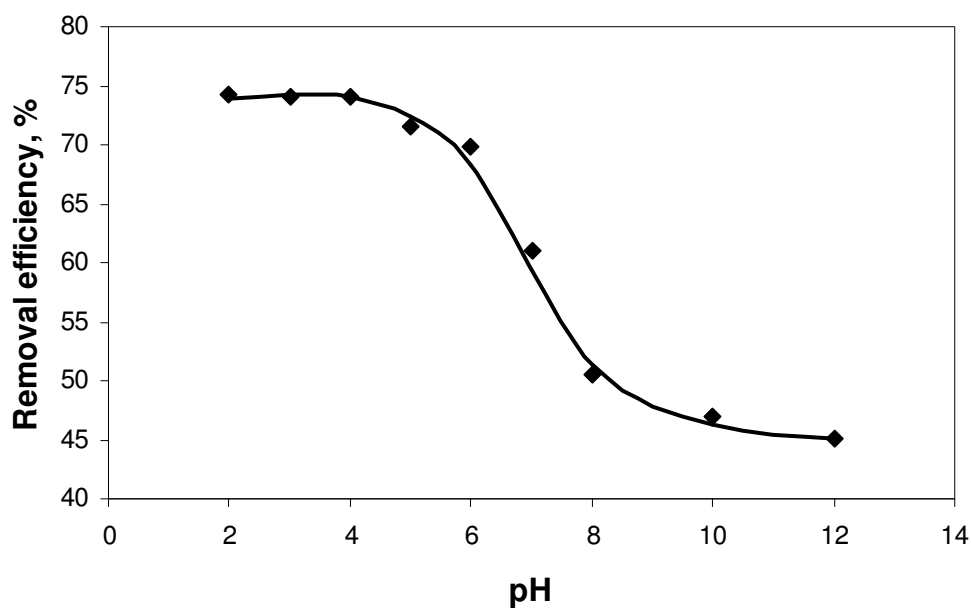


**Figure 4.8:** Variation of dye removal efficiency with solution pH

It can be observed from the above figure that dye removal efficiency decreases with increase in pH value of the solution as the dye used is an acid dye and the zeolite surface is positively charged. There could be fewer attachment sites available at higher pH due to decreased positive charge of the zeolite surface. Increasing the pH of the solution could cause the zeolite surface to decrease in positive charge, thus limiting its ability to hold onto the negatively charged dye species. The more the pH is raised, the less positive the surface becomes. Therefore, the optimum pH of the dye solution is 2–5. Hence, the pH value of 3 that has been used earlier is suitable for all the experiments.

### 4.6.3 Effect of stirrer speed

Stirring is an important parameter in adsorption phenomena, influencing the distribution of the solute in the bulk solution and the formation of the external boundary film. To study the effect of stirrer speed on the dye removal efficiency, adsorption experiments were conducted at various stirrer speeds between 0 and 400 rpm. The values of dye removal efficiency for various stirrer speeds are presented in Table 4.5 and the corresponding plot of dye removal efficiency versus stirrer speed is shown in Figure 4.9.

**Table 4.5:** Calculation of dye removal efficiency from absorbance values

<b>Stirrer speed (rpm)</b>	<b>Absorbance value (A.U.)</b>	<b>Solution concentration (mg/L)</b>	<b>Removal efficiency (%)</b>
30	0.721	11.0	45.2
75	0.550	8.4	58.2
125	0.414	6.3	68.5
200	0.335	5.1	74.5
300	0.292	4.4	77.8
400	0.275	4.2	79.1

From this figure, it is clear that with increasing agitation speed from 50 to 400 rpm, the removal efficiency increased significantly. This can be explained by the fact that increasing agitation speed reduced the film boundary layer surrounding particles, thus increasing the external film transfer coefficient, and hence the adsorption capacity. The degree of agitation reduces the boundary layer resistance and increases the mobility of the system. With agitation, the external mass transfer coefficient increases resulting in quicker adsorption of the dye molecules. It can be observed from the Figure 4.9 that agitation could improve the adsorption rate significantly. Very low values of dye removal efficiency were obtained at low stirrer speeds (<125 rpm) and the removal efficiency increased with increasing the stirrer speed. There was no significant variation in removal efficiency values at higher stirrer speeds (>300 rpm) and hence, a stirrer speed of 300 rpm was chosen to be optimal.

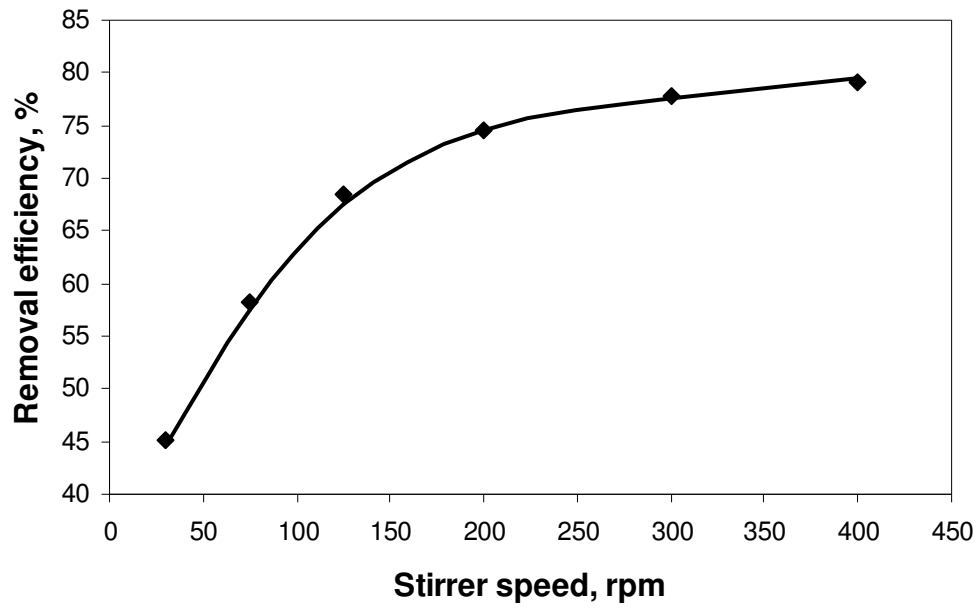


**Figure 4.9:** Variation of dye removal efficiency with stirrer speed

#### 4.6.4 Effect of dye concentration

To study the effect of initial dye concentration on the removal efficiency, adsorption experiments were conducted at various dye concentration values between 0 and 50 mg/L. The values of dye removal efficiency at various dye concentrations are presented in Table 4.6. Corresponding plot of dye removal efficiency versus initial dye concentration is shown in Figure 4.10.

**Table 4.6:** Calculation of dye removal efficiency from absorbance values

Initial dye concentration (mg/L)	Absorbance value (A.U.)	Final dye concentration (mg/L)	Removal efficiency (%)
5	0.005	0.1	98.5
10	0.153	2.3	76.7
15	0.345	5.2	65.0
20	0.585	8.9	55.5
25	0.956	14.5	41.9
30	1.220	18.5	38.2
40	1.739	26.4	33.9
50	2.282	34.7	30.6

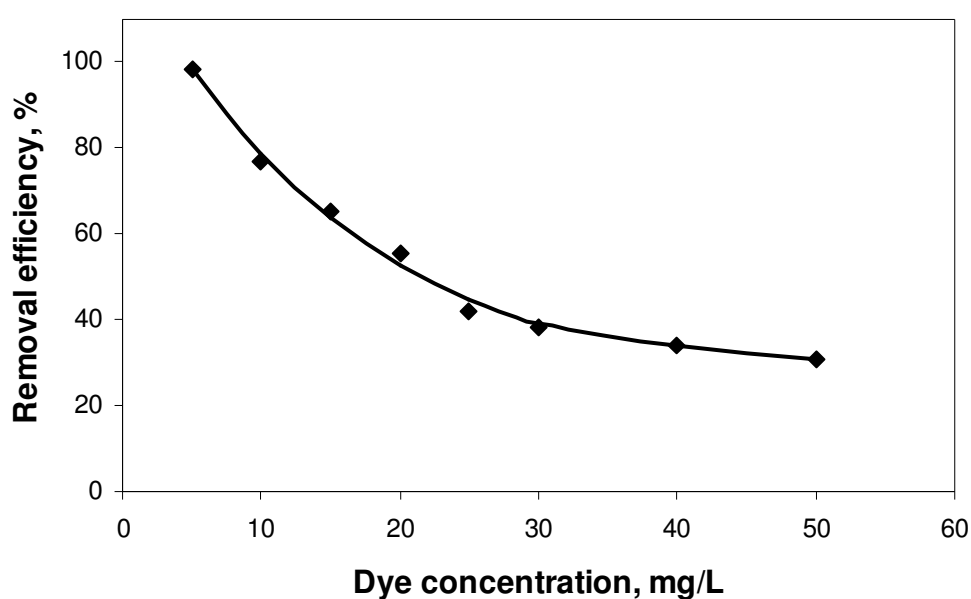


**Figure 4.10:** Variation of dye removal efficiency with initial dye concentration

From the above figure, it can be observed that the removal efficiency decreases with increasing the initial dye concentration. This indicates that the adsorption process is more effective at low concentrations of the dye solution. Similar observation was reported by Qiu et al. (2009).

#### 4.6.5 Effect of adsorption time

To study the effect of adsorption time on the dye removal efficiency, dye concentration values were noted at various time intervals between 0 and 360 min. The values of dye removal efficiency at various time intervals are presented in Table 4.7 and the corresponding plot of dye removal efficiency versus adsorption time is shown in Figure 4.11.

From this figure, it can be observed that the removal efficiency increases with increasing the time of adsorption. The slope of the curve in Figure 4.8 is decreasing with time, indicating that the adsorption rate is faster initially and it decreases with time as more amount of dye is adsorbed on the zeolite surface decreasing the availability of active adsorption sites. A similar observation was reported by Qiu et al. (2009).

**Table 4.7:** Calculation of dye removal efficiency from absorbance values

<b>Adsorption time (min)</b>	<b>Absorbance value (A.U.)</b>	<b>Solution concentration (mg/L)</b>	<b>Removal efficiency (%)</b>
0	1.330	20.2	0
30	1.079	16.4	18.9
60	0.921	14.0	30.8
90	0.806	12.2	39.4
120	0.688	10.5	48.3
180	0.541	8.2	59.3
240	0.437	6.6	67.1
300	0.367	5.6	72.4
360	0.328	5.0	75.3

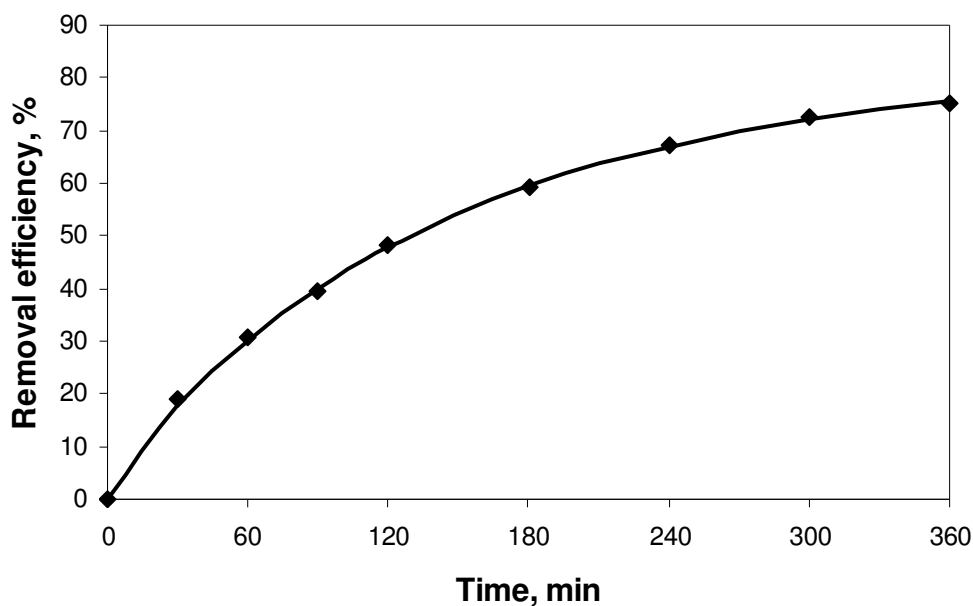


**Figure 4.11:** Variation of dye removal efficiency with time

#### 4.6.6 Effect of temperature

To study the effect of temperature on the dye removal efficiency, adsorption experiments were conducted at three different temperatures (20, 40 and 60 °C). The values of dye removal efficiency at different temperatures are presented in Table 4.6 and the corresponding plot of dye removal efficiency versus temperature is shown in Figure 4.12.

**Table 4.8:** Calculation of dye removal efficiency from absorbance values

Temperature (°C)	Absorbance value (A.U.)	Solution concentration (mg/L)	Removal efficiency (%)
20	0.354	5.4	73.4
40	0.477	7.2	64.1
60	0.684	10.4	48.6

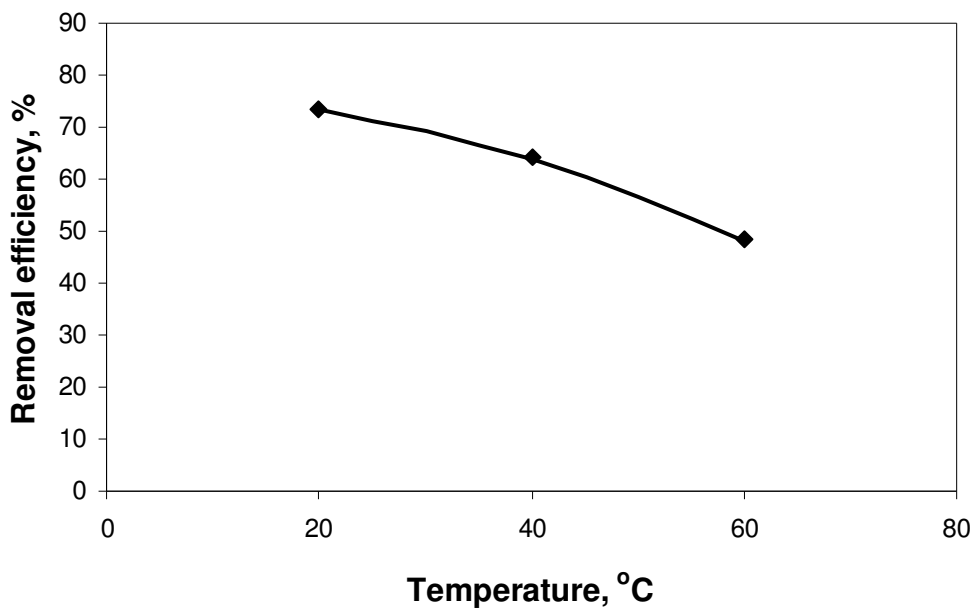


**Figure 4.12:** Variation of dye removal efficiency with temperature

From the above figure, it can be observed that the removal efficiency decreases with increasing the temperature. This indicates that adsorption is favored at lower temperatures and desorption takes place at higher temperatures due to the fact that adsorption is exothermic in nature. Similar observation was reported in several literatures (Nandi et al., 2008).

## 4.7 Thermodynamic, Kinetic and Equilibrium studies

### 4.7.1 Thermodynamics of adsorption

The thermodynamic parameters, such as the changes in the Gibbs free energy ( $\Delta G^\circ$ ), enthalpy ( $\Delta H^\circ$ ) and entropy ( $\Delta S^\circ$ ) of adsorption process are estimated from the following correlations (Eq. (4.3) and (4.4)).

The change in standard free energy ( $\Delta G^\circ$ ) at various temperatures can be estimated as follows.

$$\Delta G^\circ = -RT \ln K_d = -RT \ln \left( \frac{q_e}{C_e} \right) \quad (4.3)$$

Here, R is the universal gas constant ( $8.314 \text{ J mol}^{-1} \text{ K}^{-1}$ ), and T is the temperature in K. The relation among the thermodynamic parameters mentioned above is given by the following equation.

$$\Delta G^\circ = \Delta H^\circ - T\Delta S^\circ \quad (4.4)$$

A plot of  $\Delta G^\circ$  versus T (Figure 4.10) yields a straight line with the slope of  $-\Delta S^\circ$  and intercept of  $\Delta H^\circ$ .

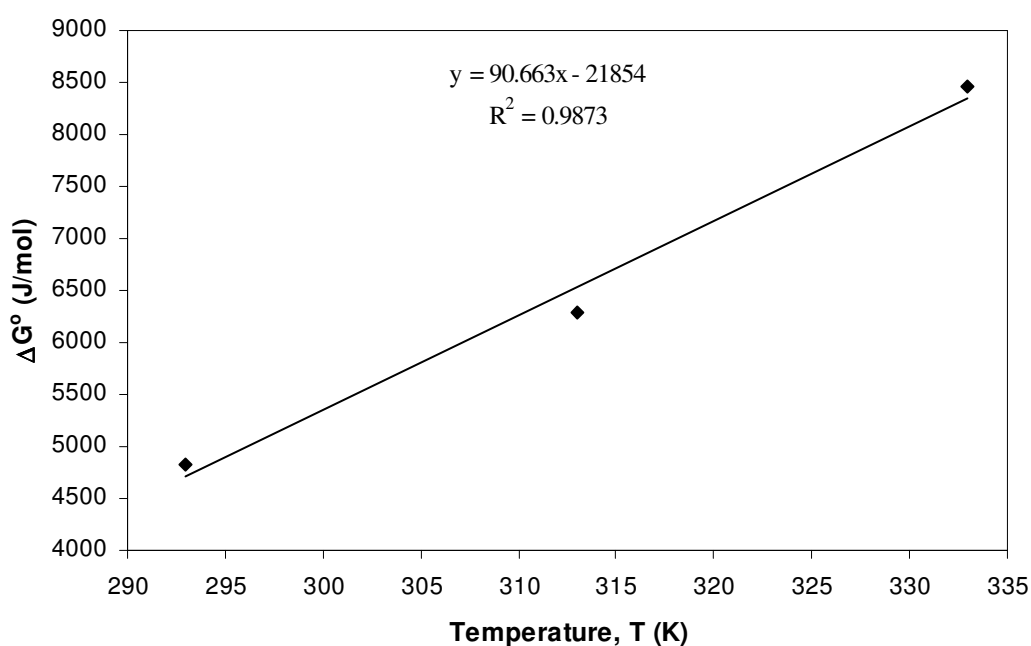


**Figure 4.13:** Plot of change in Gibbs free energy with temperature

The values of  $\Delta G^\circ$  obtained using Eq. (4.1) at the temperatures 293, 313 and 333 K are 4.8, 6.3 and 8.5 kJ/mol respectively. The values of changes in enthalpy ( $\Delta H^\circ$ ) and entropy ( $\Delta S^\circ$ ) during the adsorption process determined from the slope and intercept of Figure 4.10 are  $-21.85$  kJ/mol and  $-90.66$  J/mol  $K^{-1}$ . The negative values indicate that the adsorption process considered here is exothermic in nature and hence lower temperatures are favored.

## 4.7.2 Adsorption kinetics

Various kinetic models proposed to examine the controlling mechanism of adsorption process are a pseudo-first-order kinetic model, a pseudo-second-order kinetic model, and an intra-particle diffusion model. These three models are studied to find the best fitting model for the adsorption of Amido Black on zeolite surface.

### 4.7.2.1 Pseudo first-order kinetics

This model assumes that the rate of solute uptake is directly proportional to the concentration difference of the solute from the equilibrium saturation concentration on the adsorbent. The form of rate equation for a pseudo first-order kinetic model is as follows.

$$\frac{dq_t}{dt} = k_1(q_e - q_t) \quad (4.3)$$

Here,  $q_t$  (mg/g) is the amount of dye adsorbed after time 't' (min),  $q_e$  (mg/g) is the equilibrium dye adsorption capacity and  $k_1$  ( $\text{min}^{-1}$ ) is the pseudo first-order rate constant.

The integration of equation (4.3) with the initial condition  $q_t = 0$  at  $t = 0$  gives the following equation.

$$-\ln\left(1 - \frac{q_t}{q_e}\right) = k_1 t \quad (4.4)$$

The slope of a straight line fit to the data of  $-\ln(1 - q_t/q_e)$  versus  $t$  (as shown in Figure 4.11) passing through origin gives the value of the pseudo first-order rate constant,  $k_1$ . The experimental data was found to be fitting well with the pseudo first-order model

whose regression coefficient value is very close to 1.0. The value of the pseudo first-order rate constant,  $k_1$  as obtained from the linear curve fitting is  $0.0077 \text{ min}^{-1}$ . The value of  $q_e$  as obtained from the regression analysis ( $1.62 \text{ mg/g}$ ) is very close to the experimental value ( $1.55 \text{ mg/g}$ ) and this indicates that the pseudo first-order kinetic model can adequately represent the dye–zeolite system under consideration.

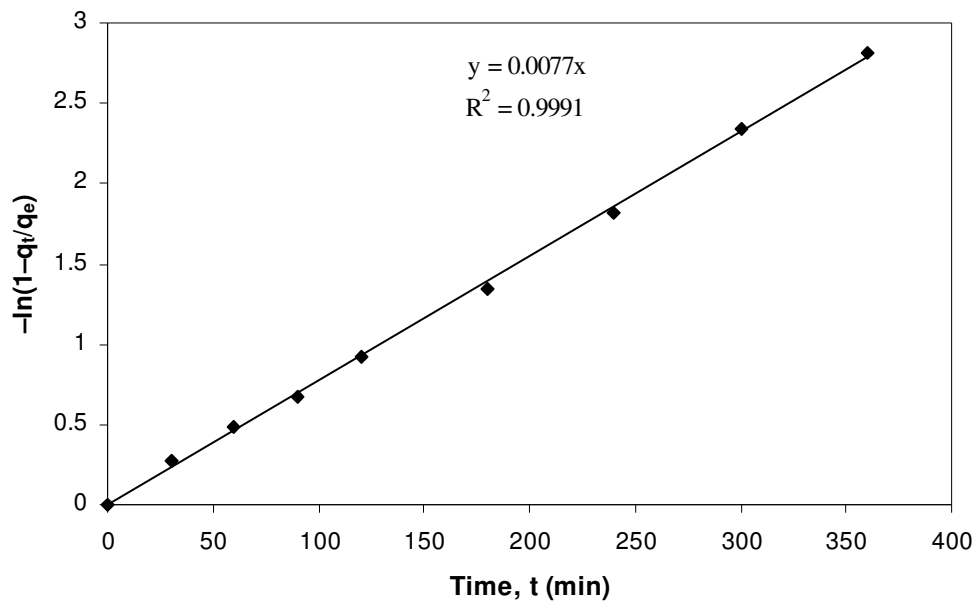


**Figure 4.14:** Pseudo first-order kinetic model for the adsorption of Amido Black dye on zeolite

#### 4.7.2.2 Pseudo second-order kinetics

This model interprets that the rate of solute uptake is directly proportional to the square of the concentration difference of the solute from the equilibrium saturation concentration on the adsorbent. The form of rate equation for a pseudo second-order kinetic model is as follows.

$$\frac{dq_t}{dt} = k_2(q_e - q_t)^2 \quad (4.5)$$

Here,  $k_2$  ( $\text{g} \cdot \text{mg}^{-1} \cdot \text{min}^{-1}$ ) is the pseudo second-order rate constant.

The integration of equation (4.5) with the initial condition  $q_t = 0$  at  $t = 0$  gives the following expression.

$$\frac{t}{q_t} = \frac{1}{k_2 q_e^2} + \frac{t}{q_e} \quad (4.6)$$

The values of  $q_e$  and  $k_2$  can be obtained from the slope and intercept of a straight line fit to the data of  $t/q_t$  versus  $t$  (as shown in Figure 4.12). The slope and intercept obtained from the graphical analysis are 0.4635 and 67.488 and the values of  $q_e$  and  $k_2$  thus obtained are 2.1575 mg/g and 0.0032 g.mg<sup>-1</sup>.min<sup>-1</sup> respectively. Although, the regression coefficient value is close to 1.0, the value of  $q_e$  (2.15 mg/g) deviates significantly from experimental observation (1.55 mg/g). Therefore, the pseudo second-order kinetic model is not appropriate for the dye–zeolite system considered in this study.

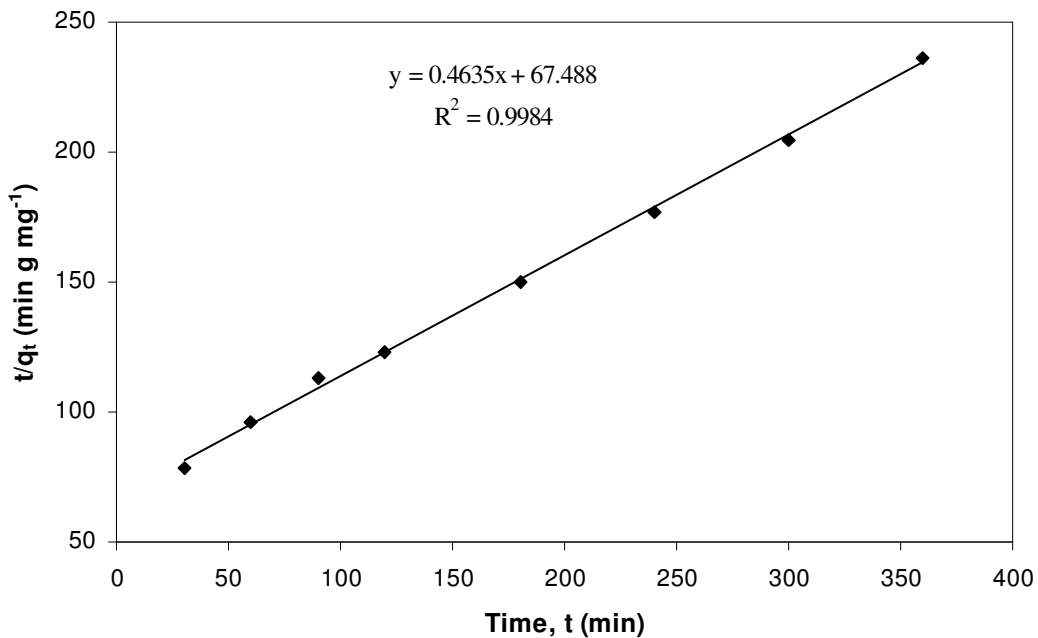


**Figure 4.15:** Pseudo second-order kinetic model for the adsorption of Amido Black 10B dye on zeolite

#### 4.7.2.3 Intra-particle diffusion model

This model considers the bulk diffusion, film diffusion, pore diffusion in addition to the adsorption phenomenon. The form of rate equation for the intra-particle diffusion model is as follows.

$$q_t = k_i t^{1/2} + C_i \quad (4.7)$$

Here,  $k_i$  ( $\text{mg/g}\cdot\text{min}^{-0.5}$ ) is the intra-particle diffusion rate constant and  $C_i$  ( $\text{mg/g}$ ) is the intercept, which corresponds to the boundary layer thickness. The values of  $k_i$  and  $C_i$  can be determined directly as the slope and intercept of the linear plot of  $q_t$  versus  $t^{0.5}$ . The values of  $k_i$  and  $C_i$  obtained from the graph (Figure 4.13) are  $0.0836 \text{ mg/g}\cdot\text{min}^{-0.5}$  and  $0.0167 \text{ mg/g}$  respectively.

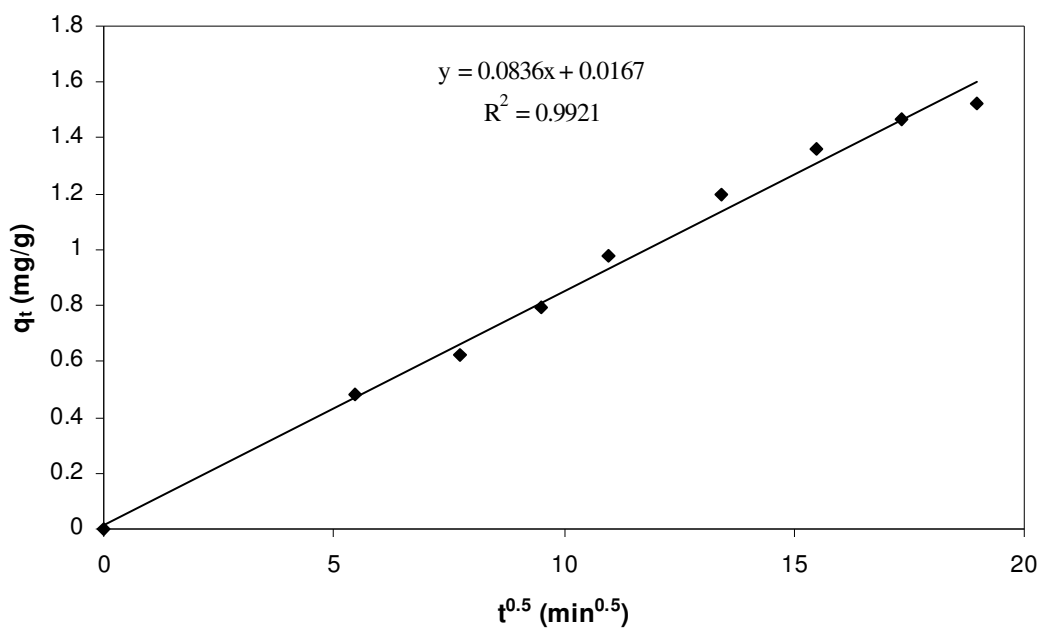


**Figure 4.16:** Intra-particle diffusion model for the adsorption of Amido Black 10 B dye on zeolite

Although, the regression coefficient value is close to 1.0, it is still less than that obtained for the pseudo first-order kinetic model.

### 4.7.3 Equilibrium adsorption isotherms

Adsorption isotherms describe the nature of interaction between the adsorbent and the adsorbate molecules at equilibrium. The two most common types of adsorption isotherms are Langmuir and Freundlich isotherms. The parameters of these equilibrium isotherms are useful in the optimum design of adsorption systems. The Langmuir isotherm simply assumes that there is a homogeneous distribution of active sites (binding sites) on the surface of the adsorbent, which adsorb a single molecular layer of adsorbate molecules with no interaction between the adsorbed molecules. The Langmuir isotherm equation is given by.

$$q_e = \frac{Q_m K_L C_e}{1 + K_L C_e} \quad (4.8)$$

Where  $C_e$  (mg/L) and  $q_e$  (mg/g) are the liquid phase concentration and solid phase concentration of adsorbate at equilibrium, and  $Q_m$  (mg/g) corresponds to the maximum adsorption capacity of the adsorbent where as  $K_L$  (L/mg) corresponds to the equilibrium adsorption constant of the Langmuir isotherm.

The linearized form of equation (4.8) is as follows.

$$\frac{C_e}{q_e} = \frac{1}{Q_m K_L} + \frac{C_e}{Q_m} \quad (4.9)$$

The values of  $Q_m$  and  $K_L$  can be determined from the slope and intercept of a linear curve fit to the plot of  $C_e/q_e$  versus  $C_e$  (shown in Figure 4.14).

Further, the equilibrium adsorption intensity ( $R_L$ ), which indicates the type of adsorption, is defined as follows.

$$R_L = \frac{1}{1 + K_L C_i} \quad (4.10)$$

Here,  $C_i$  is the initial dye concentration (mg/L) in the solution. For a favorable adsorption,  $R_L < 1$ ; for a linear adsorption,  $R_L = 1$ ; and for an unfavorable adsorption,  $R_L > 1$ . A plot of  $R_L$  versus  $C_i$  is shown in Figure 4.15. From this figure, it can be observed that the adsorption process is more favorable at higher concentrations of dye solution.

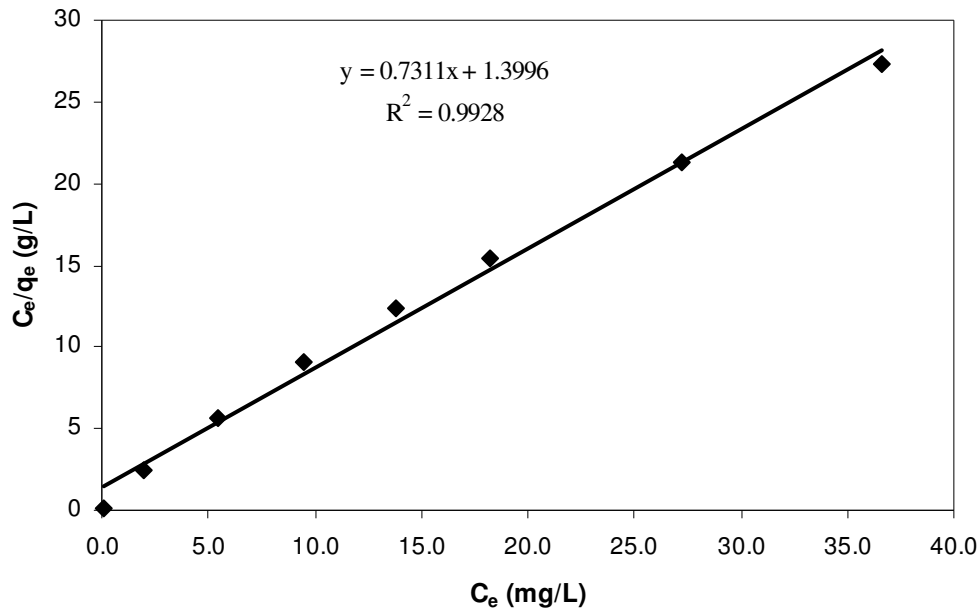


**Figure 4.17:** Plot of  $C_e/q_e$  versus  $C_e$  for the estimation of Langmuir isotherm constants

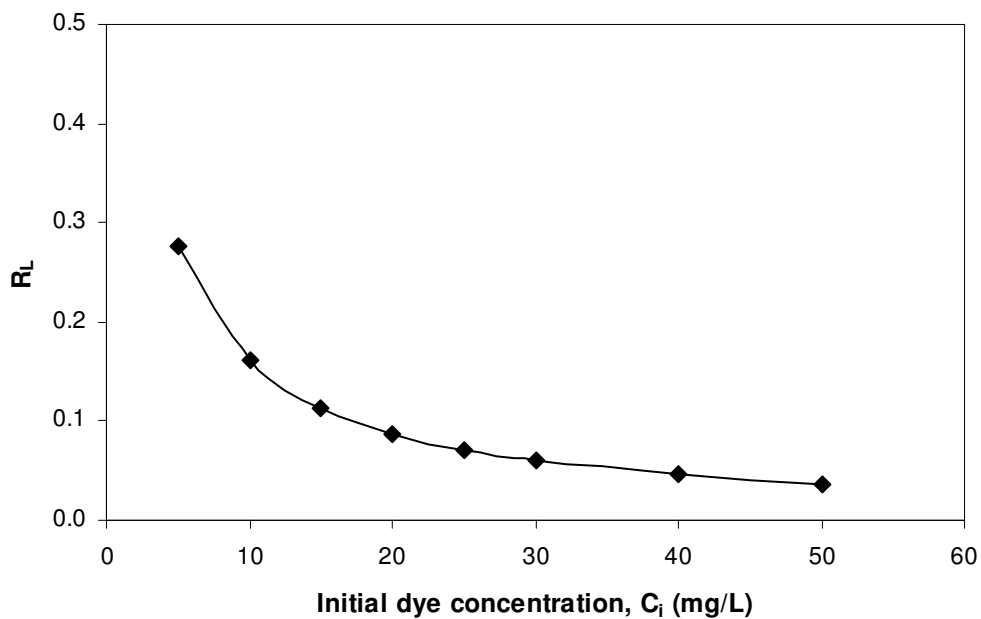


**Figure 4.18:** Variation of equilibrium adsorption intensity ( $R_L$ ) with initial dye concentration ( $C_i$ )

The Freundlich isotherm model is an exponential equation, which applies to heterogeneous systems with interaction between adsorbed molecules and is not restricted to the formation of a monolayer. This model assumes that as the adsorbate concentration increases, the concentration of the adsorbate on the adsorbent surface

also increases and correspondingly that sorption energy exponentially decreases on completion of the sorption centers of an adsorbent. The well-known expression for the Freundlich model is as follows.

$$q_e = K_F C_e^{1/n} \quad (4.11)$$

Where, 'K<sub>F</sub>' is the Freundlich constant [(mg/g).(mg/L)<sup>-n</sup>] related to the bonding energy, and n is the heterogeneity factor (exponent). Here, 'n' is a measure of the deviation from linearity of the adsorption and indicates the degree of non-linearity between the solution concentration and the adsorption rate. A power-law model curve fit to the data of q<sub>e</sub> versus C<sub>e</sub> could yield the values of K<sub>F</sub> and n.

Both the isotherms for the dye–zeolite system at 20°C and a pH of 4 are shown in Figure 4.16. From this figure, it can be observed that the equilibrium adsorption between Amido Black dye and zeolite can better be represented by Freundlich isotherm than the Langmuir isotherm.

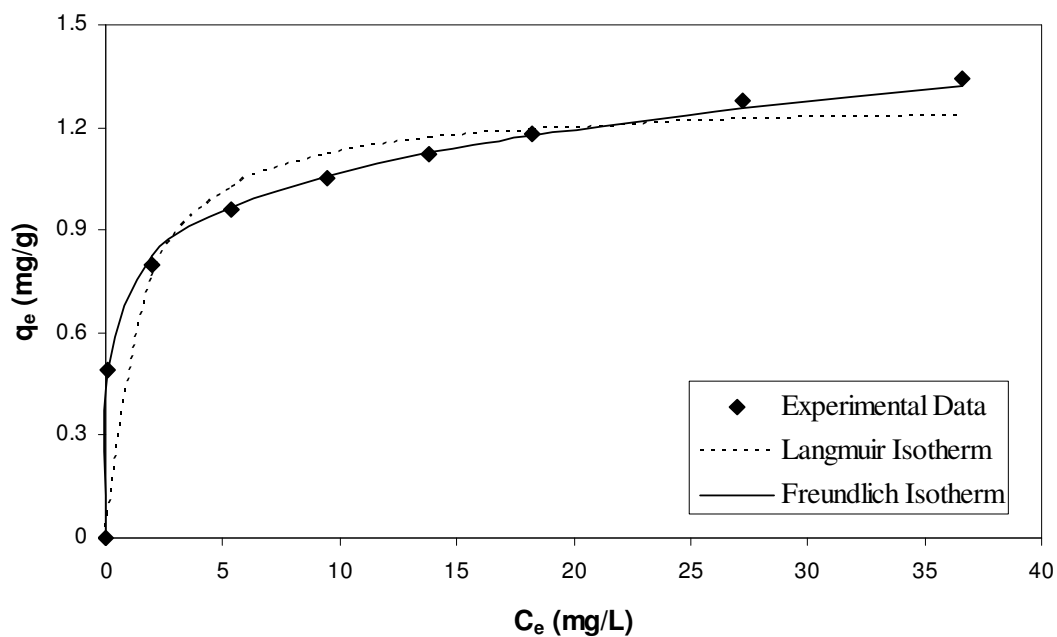


**Figure 4.19:** Equilibrium isotherms for the adsorption of Amido Black on zeolite

The trend observed in the experimental data is very close to the Freundlich isotherm but it is deviating considerably from the Langmuir isotherm. This indicates that the adsorption process is of multi-layer type with some interaction among the adsorbed molecules. The evaluated model parameters for both Langmuir and Freundlich

adsorption isotherms are presented in Table 4.7. Corresponding values of correlation coefficients ( $R^2$ ) are also shown in the table.

**Table 4.9:** Equilibrium parameters for Langmuir and Freundlich adsorption isotherms

<b>Langmuir isotherm</b>		<b>Freundlich isotherm</b>	
<b>Parameter</b>	<b>Value</b>	<b>Parameter</b>	<b>Value</b>
$Q_m$	1.3678	$K_F$	0.7353
$K_L$	0.5224	$1/n$	0.1625
$R^2$	0.9928	$R^2$	0.9976

#### 4.8 Comparison of zeolite performance with a commercial adsorbent

The removal efficiency of the synthesized zeolite (ZX) is compared with a commercially available adsorbent (13X). It can be observed from the figure (Figure 4.7) that the zeolite synthesized in laboratory (ZX) performs three times better than the commercial adsorbent (13X). The maximum dye removal efficiency obtained for the synthesized zeolite is 75.3% and the removal efficiency for the commercial adsorbent is only 27.2%.

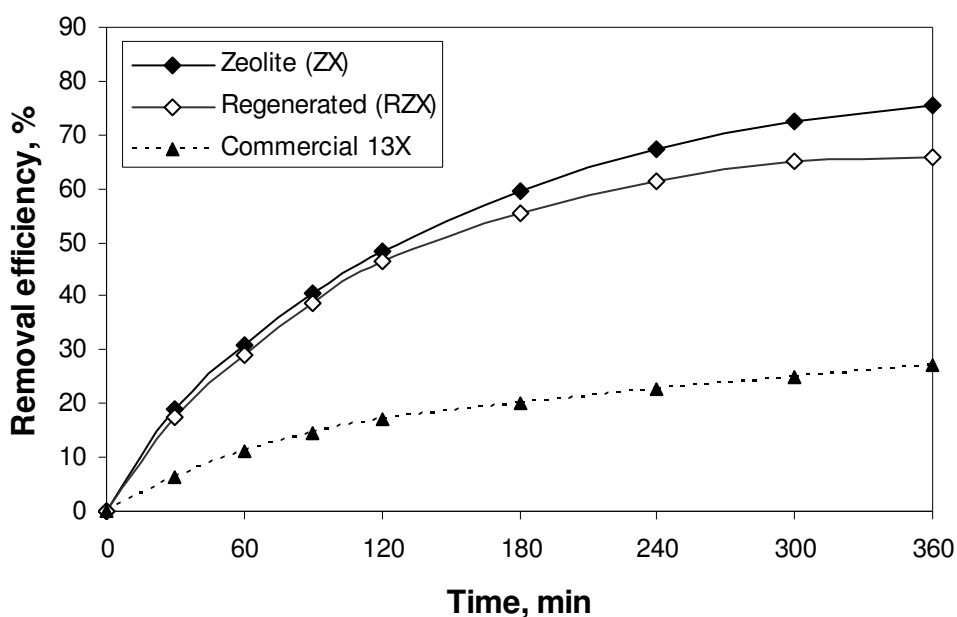


**Figure 4.20:** Comparison of dye removal efficiency over synthesized zeolite (ZX) and commercial zeolite (13X).

## Chapter 5

### CONCLUSIONS AND FUTURE WORK

---

The following conclusions have been derived from the experimental analysis carried out so far.

- Zeolite has been synthesized from low-cost raw material, i.e. fly ash.
- The prepared zeolite has been successfully applied for the adsorptive removal of Amido Black 10 B dye from its aqueous solutions.
- The prepared fly ash based zeolite is found to be more effective than the natural zeolite *clinoptilolite* presented in the literature (Qiu et al., 2009).
- The optimum zeolite concentration obtained from the experimental studies for Amido Black is 100 g/L.
- $\lambda_{\max}$  for Amido Black 10B dye solution was found to be 618 nm.
- Optimal pH value obtained is 3.
- Optimal stirrer speed is 300 rpm.
- Removal efficiency decreases with increasing the initial dye concentration.
- Removal efficiency increases with increasing the adsorption time.
- Adsorption process is exothermic and is favored at low temperatures.
- Experimental data matches well with the pseudo-first-order kinetics.
- Experimental data matches well with the Freundlich isotherm than the Langmuir isotherm.

Most important observation in this work is that the zeolite synthesized from fly ash could act as a very effective adsorbent for the removal of Amido Black dye. The removal efficiency increased with increasing the zeolite concentration significantly and reached a value as high as 74% at lower concentrations (up to 100 g/L) where as no significant change was observed at higher concentrations.

Work done so far includes the preparation of zeolite and studying the effect of various parameters on the removal of Amido Black 10B dye. However, there is a lot of scope for further research in this area. Some of the objectives that can be studied in future are as follows.

1. Studying the performance of the prepared zeolite for the removal of other important dyes used in the industry.

2. Using the prepared zeolite for industrial wastewater treatment in continuous mode (fixed bed or fluidized bed studies).
3. Removal of heavy metals from water by adsorption with the prepared zeolite.

As the project has already been completed, the rest of this work is recommended as future work for the next batch of students.

## References

- Ahmad, R., Kumar, R., (2010) "Conducting Polyaniline/Iron Oxide Composite: A Novel Adsorbent for the Removal of Amido Black 10B,". *J. Chem. Eng. Data* 55, 3489–3493
- Ajmal Mohammad, Ali Mohammad, Rehana Yousuf and Anees Ahmad (1998) "Adsorption behaviour of Cadmium, Zinc, Nickel and Lead from aqueous solutions by Mangifera Indica seed shell", *Indian J. Environ. Hlth.*, 40 (1), 15-26.
- Al-Ghouti, M.A., Khraisheh, M.A.M., Allen, S.J., Ahmad, M.N., (2003). "The removal of dyes from textile wastewater: a study of the physical characteristics and adsorption mechanisms of diatomaceous earth." *Journal of Environmental Management*, 69 (3), 229–238.
- Alok Mittal, Arti Malviya, Dipika Kaur, Jyoti Mittal, Lisha Kurup (2007), "Studies on the adsorption kinetics and isotherms for the removal and recovery of Methyl Orange from wastewaters using waste materials". *Journal of Hazardous Materials*, 148, (1-2), 229-240.
- Atun G., Hisarh G., Kurtoglu A.E., Ayar N., (2011); "A comparison of basic dye adsorption onto zeolitic materials synthesized from fly ash"; *Journal of Hazardous materials*. 187: 562-573.
- Bhatnagar A., Minocha A.K., (2006), "Conventional and non-conventional adsorbents for removal of pollutants from water- a review"; *Indian Journal of Chemical Technology* 13: 203-217.
- Breck D.W., 1974; *Zeolite molecular sieves*, J. Wiley, New York.
- Chakraborty, S., Purkait, M.K., DasGupta, S., De, S., and Basu, J.K. (2003) "Nanofiltration of textile plant effluent for color removal and reduction in COD." *Sep. Purif. Technol.*, 31: 141–151.
- Chang H.L. and Shih W.H., (1998) "A general method for the conversion of fly ash into zeolites as ion exchangers for Cesium". *Ind. Eng. Chem.* 37: 71-78.

Chang, H.L. and Shih, W.H., (2000) “Synthesis of zeolite A and X from fly ashes and their ion exchange behaviours with Cobalt ions”; *Ind. Eng. Chem.* 35:4185–4191.

Eilbeck, W.J. and Mattock, G. (1985). *Chemical Processes in Wastewater Treatment*; John Wiley and Sons, Inc.: Chichester.

Fatma, C., Dursun, O., Ahmet, O., and Ayla, O. (2006) “Low cost removal of reactive dyes using wheat bran”. *J. Haz. Mat.*, 146(1–2):408–416.

Fukui K., Nishimoto T., Takiguchi M. and Yoshida H., (2003) “Effects of NaOH concentration on zeolite synthesis from fly ash with a hydrothermal treatment method”; *J. Soc. Powder Technology Japan.* 40:497–504.

Gong, R., Ding, Y., Li, M., Yang, C., Liu, H., and Sun, Y. (2005). “Utilization of powdered peanut hull as biosorbent for removal of anionic dyes from aqueous solution.” *Dyes Pigments*, 64: 187–192.

Grutzeck M.W. and Siemer D.D., (1997) “Zeolite synthesized from class F fly ash and Sodium Alluminate Slurry”; *J. Am. Ceram. Soc.* 80:2449-2453.

Gülten Atun, Gül Hisarlı, Ayşe Engin Kurtoğlu, Nihat Ayar (2011) “A comparison of basic dye adsorption onto zeolitic materials synthesized from fly ash”. *Journal of Hazardous Materials*, 187(1-3):562–573.

Gupta, V.K., Suhas, Ali, I., Saini, V.K., 2004. “ Removal of rhodamine B, fast green, and methylene blue from wastewater using red mud, an aluminum industry waste’’. *Industrial & Engineering Chemistry Research* 43 (7), 1740–1747.

Hao, O.J., Kim, H., and Chiang, P.C. (2000) Decolorization of wastewater. *Crit.Rev. Environ. Sci. Technol.*, 30: 449–505.

Henmi T., 1987b; “Increase in cation exchange capacity of coal fly ash by alkali treatment”; *Clay Science* 6:277–282.

J.X. Lin, S.L. Zhan, M.H. Fang, X.Q. Qian, H Yang (2008), “Adsorption of basic dye from aqueous solution onto fly ash”. *Journal of Environmental Management*, 87, (1):193–200.

Jian-Hui Sun, Sheng-Peng Sun, Guo-Liang Wang, Li-Ping Qiao (2007), “Degradation of azo dye Amido black 10B in aqueous solution by Fenton oxidation process”; *Dyes and Pigments*. 74(3): 647–652.

Vasanth K., V. Ramamurthi, S. Sivanesan (2005), “ Modeling the mechanism involved during the sorption of methylene blue onto fly ash”. *Journal of Colloid and Interface Science*, 284, (1) 14-21.

Ledakowicz, S., Solecka, M., and Zylla, R. (2001) “Biodegradation, Decolourization and detoxification of textile wastewater enhanced by advanced oxidation processes.” *J. Bio-Technol.*, 89: 175–184.

Lǔ H., Wang B. and Ban Q., 2010; “Defluoridation of drinking water by zeolite NaP1 synthesized from coal fly ash”; *Energy Sources Part A* 32:1509-1516.

Manju, G.N. and T.S. Anirudhan (1997). “Use of Coconut fibre pith-based Pseudo Activated carbon for Chromium (VI) removal” , *Indian J. Environ. Hlth.*, 39 (4), 289-298.

Markovska, L, Mesko V, Minceva, M (1999) “Two resistance mass transfer model for the adsorption of basic dyes from aqueous solution on natural zeolite”; *Bulletin of the Chemists and Technologists of Macedoni*. 18 (2), 161-169.

Mehmet, U D, Levent, C, Papageorgiou, S K., Fotis K. K (2011), “Methylene blue adsorption on activated carbon prepared from *Posidonia oceanica* (L.) dead leaves: Kinetics and equilibrium studies”;

Mohd. R, Othman S, Rokiah H, Anees, A (2010), “Adsorption of methylene blue on low-cost adsorbents: A review”. *Journal of Hazardous Materials*, 177(1-3): 70.

Nandi, B.K., Goswami, A., Das, A.K., Mondal, B. and Purkait, M.K. (2008), “Kinetic and Equilibrium Studies on the Adsorption of Crystal Violet Dye using Kaolin as an Adsorbent”, *Separation Science and Technology*, 43: 1382–1403.

Nourali Mohammadi, Hadi Khani, Vinod Kumar Gupta, Ehsanollah Amereh, Shilpi Agarwal (2011), “Adsorption process of methyl orange dye onto mesoporous carbon material–kinetic and thermodynamic studies” *Journal of Colloid and Interface Science*, 362(2): 457-462.

Nugteren H.W., Hallman G.G., Janssen-Jurkovicova M., (1995); *Proceedings of international ash utilization symposium* 224.

Ohja, K., Pradhan N.C., Samanta A.N., 2004; “Zeolite from fly ash: Synthesis and Characterisation”; *Bull. Mater. Sci.* 27:555-564.

Ozbayrak, O., Alpat S.K., Alpat S., Akcay H., 2004; “ The investigation of adsorption properties of phenothiazine derivatives on natural clinoptilolite”; *Adnan Menderes University, 4th AACD Congress, 29 Sept-3 Oct., Kuşadası-AYDIN, TURKEY Proceedings Book* 170.DOC

Peng, Liu, Liuxue, Z. (2007), “Adsorption of dyes from aqueous solutions or suspensions with clay nano-adsorbents”; *Separation and Purification Technology, Volume 58, Issue 1, Pages 32-39.*

Pollock, M. (1973), “Neutralizing dye-housewastes with flue gases and decolorizing with fly ash”. *Am. Dyestuff Rep.*, 62: 21–23.

Purkait, M.K., DasGupta, S., and De, S. (2003), “Removal of dye from wastewater using micellar enhanced ultrafiltration and recovery of surfactant.” *Sep. Purif. Technol.*, 37: 81–92.

Purkait, M.K., Das Gupta, S., and De, S. (2006), “Micellar, enhanced ultrafiltration of dye using hexadecyl pyridinium chloride.” *J. Hazard. Mat.*, B136: 972–977.

Purkait, M.K., Maiti, A., DasGupta, S., and De, S. (2007) Removal of congo red using activated carbon and its regeneration. *J. of Haz. Mat.*, Vol 145(1–2), pp 287–295.

Qiu, M., Qian, C., Xu, J., Wu, J., Wang, G. (2009), “Studies on the adsorption of dyes into clinoptilolite”, *Desalination* 243, 286–292.

Runping Han, Jingjing Z., Pan H, Yuanfeng W., Zhenhui Z, Mingsheng T., (2009), “Study of equilibrium, kinetic and thermodynamic parameters about methylene blue adsorption onto natural zeolite” *Chemical Engineering Journal*, 145(3):496–504.

Ruthven, D., (1984) *Principles of Adsorption and Adsorption Processes*, John Wiley & Sons, New York.

Senthilkumar, S., Perumalsamy, M., Prabhu, H.J., Decolourization potential of white-rot fungus *Phanerochaete chrysosporium* on synthetic dye bath effluent containing Amido black 10B, *Journal of Saudi Chemical Society*, In Press, doi:10.1016/j.jsocs.2011.10.010.

Shaobin, Wang, Lin Li, Hongwei Wu, Z.H. Zhu (2005), “Unburned carbon as a low-cost adsorbent for treatment of methylene blue-containing wastewater”. *Journal of Colloid and Interface Science*, 292, (2):336–343.

Shaobin, W, Qing Ma, Zhu Z.H. (2008), “Characteristics of coal fly ash and adsorption application”, *Fuel*, 87(15-16), 3469–3473.

Suhong Chen, Jian Zhang, Chenglu Zhang, Qinyan Yue, Yan Li, Chao Li (2010), “Equilibrium and kinetic studies of methyl orange and methyl violet adsorption on activated carbon derived from *Phragmites australis*”; *Desalination*, 252,(1-3) :149–156.

Venkat, S.M., Indra, D.M., and Vimal, C.S. (2006). “ Kinetic and equilibrium isotherm studies for the adsorptive removal of Brilliant Green dye from aqueous solution by rice husk ash.” *J. of Env. Manage.*, (Available online).74,(3): 647–652.

Yamin Y, Abd. Hafiz Abd. Malek, and Siti Mariam S, (2009) “Removal of Amido Black Dye from Aqueous Solution by Uncalcined and Calcined Hydrotalcite” *AIP Conf. Proc.* 1136: 533–539.

Youji, Li, Xiaodong, Li, Junwen, L., Jing Y., (2006), “Photocatalytic degradation of methyl orange by TiO<sub>2</sub>-coated activated carbon and kinetic study”, *Water Research*, 40(6):1119–1126.

Yunus, O., (2006) “Kinetics of adsorption of dyes from aqueous solution using activated carbon prepared from waste apricot”. *J. Hazard. Mat.*, B137:1719–1728.